Single-Atom Catalysts: A Sustainable Pathway for the Advanced Catalytic Applications

Baljeet Singh,* Vikas Sharma, Rahul P. Gaikwad, Paolo Fornasiero, Radek Zbořil, and Manoj B. Gawande*

A heterogeneous catalyst is a backbone of modern sustainable green industries; and understanding the relationship between its structure and properties is the key for its advancement. Recently, many upscaling synthesis strategies for the development of a variety of respectable control atomically precise heterogeneous catalysts are reported and explored for various important applications in catalysis for energy and environmental remediation. Precise atomic-scale control of catalysts has allowed to significantly increase activity, selectivity, and in some cases stability. This approach has proved to be relevant in various energy and environmental related technologies such as fuel cell, chemical reactors for organic synthesis, and environmental remediation. Therefore, this review aims to critically analyze the recent progress on single-atom catalysts (SACs) application in oxygen reduction reaction, oxygen evolution reaction, hydrogen evolution reaction, and chemical and/or electrochemical organic transformations. Finally, opportunities that may open up in the future are summarized, along with suggesting new applications for possible exploitation of SACs.

1. Introduction

Our society is facing massive challenges to ensure a sustainable future. For instance, numerous strategies exist or are under investigation to guarantee progress based on more energy-efficient technology, able to produce value-added chemicals with low energy and mass requirements, in a circular economy concept that includes dramatic reduction of the generation of waste and pollutants.[1,2] In order to achieve these goals, it is of fundamental importance to design new catalysts that enable new benign routes to produce/store and convert renewable energies and to obtain chemicals from waste.[3–5] We need to design new chemical pathways that replace traditional petrochemical-based routes, considering new platform molecules, possibly derived by renewable resources such as agriculture/municipal wastes. This transition must fully involve the energy sector, with the entire redefinition of the pool of energy vectors for transportations, building heating systems, and power production. As the burning of fossil fuels and biomass are not anymore compatible with the dramatic increasing air pollution and global warming.

To achieve all these targets, we will need to design nontoxic, earth-abundant, and less-expensive, highly efficient, and selective catalysts that can work under mild reaction conditions without producing significant waste.[6,7] Catalytic activity and selectivity are enabled via the many factors such as accessibility of active sites, interaction with the surface, i.e., varying support and coordinating sphere, composition of metals (bimetallic and many-metallic), size and shape; and chemical states of active sites which can to tailored via developing 2D catalyst[8–10] or via developing single atomic sites stabilized on hollow

surfaces.[11,12] For example, Somorjai and co-workers controlled the selectivity of dendrimer-encapsulated Au nanoclusters (Au-G4OH/SBA-15) by varying the dendrimer properties which is in a similar strategy used by ligand modification in a homogeneous catalyst.[13] In another example to tune the selectivity, Ag nanowire was found more selective for ethylene epoxidation reaction compared to spherical catalyst.[14]

However, heterogeneous catalysis is essentially a surface process, and therefore it is limited by surface accessibility. The catalyst development therefore involves a decrease in size of the active phase, as the reduction in particle size implies an increase in surface-to-volume ratio. This process has gained enormous advancement by the advent of nanoscience and nanotechnology, more recently has found a revolutionary approach in the development of single-atom catalysts (SACs).[15] In 2003, Saltsburg and Flytzani-Stephanopoulos investigated Au and Pt in an ionic forms which were strongly associated with the surface of ceria and responsible for the water-gas shift reaction. They reported that Pt or Au nanoparticles on the surface of ceria did not participate in the catalysis, the ionic form of Au or Pt on the surface of ceria has functioned as SACs.[16] Subsequently, in 2006, Bashyam and Zelenay investigated cobalt and iron porphyrins complex which was pyrolyzed under controlled temperatures to produce M–N_x species which were suggested as an active site for oxygen reduction reaction (ORR).[17] However, even before 2003, the role of trace metal existence in organic catalysis cannot be completely ruled out which were the single metallic active sites in homogeneous form.[18,19] In the subsequent years the advancement in characterization tools made it possible to confirm the existence of single-atom (SA). Later in 2011, first the term SACs was introduced by Zhang and co-workers, where they have prepared SACs by using Pt metal on FeO_x support that exhibited high catalytic activity and stability for CO oxidation in a H_2-rich stream.[20] A metal SA can occupy a different location or defect in the host framework. These trap sites can help SA to get stabilize during catalytic cycles and make them leach proof.

Figures of merit that allow evaluation of performances and sustainability of heterogeneous catalyst includes selectivity, conditions, activity expressed in terms of turnover number (TON) and turnover frequency (TOF), and stability.[21] A promising catalyst must simultaneously be characterized by high conversion with high selectivity, ideally working under mild conditions (low temperature and pressure). Furthermore, it should possess long term thermal and chemical stability. The accessibility of the active sites is highly desired for the overall performance of catalysts and hence porosity should not be compromised during the operation. Catalytic activities are also influenced by the interaction of heterogeneous surfaces primarily with the reactant, product, and intermediates which depends on the catalytic reaction conditions. For a good outcome, the interaction of different components of the catalytic process with the catalyst surface should be self-sufficient to propagate a reaction, which is hard to estimate quantitatively. Surface nonuniformity also makes it more difficult to understand the interaction between the active sites and reactants at the molecular level. And these effects may play an important role in controlling the catalysis in a broad range of reaction conditions. Hence, to achieve a high selectivity, a uniform catalytic surface needs to be designed for the production of targeted reaction products. However, nanocatalyst surfaces are highly challenging to controls but then again SACs may lead to highly selective catalysts.

SACs can provide an efficient and highly active catalyst for sustainable and greener chemical industries. SACs are the base of biological and natural catalytic processes; and organometallic SA catalysts already have revolutionized industries.[22–24] However, these issues associated with the homogenous lead to the development of SACs.[25] SACs not only maximized the utilization of the active sites but also increases efficiency, reduce the metal uses, also change the selectivity. However, many challenges associated with the SACs are needed to address to make the catalytic process more sustainable and benign.[26–28] Interest in developing SACs is continuously growing and becoming a new frontier in heterogeneous catalysis.[29,30] The enrolment and development of SACs will have a profound impact on energy (generation and storage), environment protection, and chemical manufacturing from waste resources.[31] There are several methods reported for the preparation of SACs such as impregnation (wet and dry impregnation),[32] coprecipitations,[33] atomic layer deposition (ALD),[34] by carbonization of MOF in the presence of an inert atmosphere,[35] and wet-chemical synthesis.[36]

Aggregation of metal atoms during the synthesis is a major challenge for large-scale production, however, atomic level dispersion can be controlled using expensive technologies such as ALD[37] and mass-selected soft landing.[38] Nevertheless, the use of these techniques is still limited to large-scale production. The use of metal nanoparticles as a precursor for preparing SACs under thermal treatment was recently demonstrated. A facile thermal emitting strategy from bulk nanoparticles to SA could be an alternative and appealing solution.[39] Thermal vaporized Pt atom can be stabilized by N_4 atoms on defected graphene. Few methods for the preparation of SACs are summarized in **Figure 1**.

Stabilization of SA is a major challenge that can be achieved by optimum coordination with the neighboring heteroatoms. In the direction of the synthesis of stable SACs, a strong covalent metal–support interaction can yield high metal loading on the metal oxide surface. The thermally stable Pt-SA are either trapped by already deposited Pt atoms or PtO_2 formed during high-temperature calcination.[46] A simple organic molecule chelating approach can also be used for the atomic dispersion of an SA on host support. For example, ethanolamine can chelate Pt cations and later can be removed by a rapid thermal treatment in an inert atmosphere.[47] Many advanced characterization techniques including high angle annular dark-field scanning tunneling electron microscopy,[48] scanning tunneling microscopy,[49] X-ray absorption microscopy,[50,51] infrared spectroscopy[52] are essential to identify highly active and stable SACs at large scale for industrial applications.[53] Theoretical calculations by density functional theory (DFT),[54] primarily applied to the ideal system which can help in understanding the catalytic phenomena at the atomic or molecular level. Apart from all, most in-built approach for the characterization of an SA is direct imaging at the atomic scale using X-ray absorption near edge structure[55] and extended X-ray absorption fine structure[56] which can provide information relating to the nature of neighboring atomic sites and corresponding oxidation states.
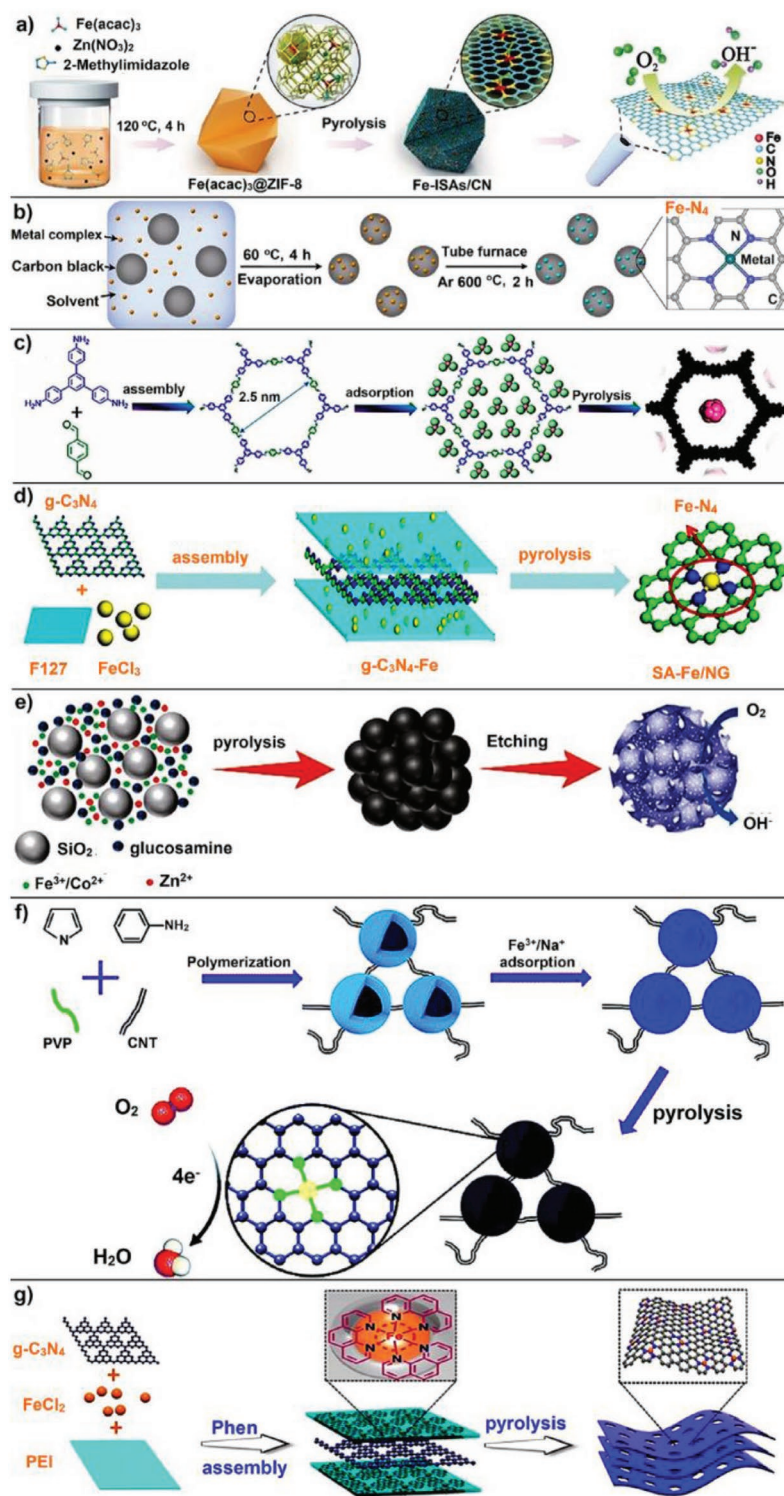
Figure 1. Various methods of preparation of SACs. a) Zeolitic imidazolate framework-based synthesis. Reproduced with permission.[35] Copyright 2017, John Wiley and Sons. b) Ligand mediated method for large scale synthesis. Reproduced with permission.[40] Copyright 2019, Nature Publishing Group. c) COF initiated the synthesis of SA catalyst. Reproduced with permission.[41] Copyright 2019, American Chemical Society. d) Using C_3N_4 as support. Reproduced with permission.[42] Copyright 2018, Proceedings of the National Academy of Sciences. e) Using SiO_2 as a hard template. Reproduced with permission.[43] Copyright 2018, John Wiley and Sons. f) Polymerization process for SACs preparation on hollow carbon. Reproduced with permission.[44] Copyright 2019, Royal Society of Chemistry. g) Using C_3N_4 as support and PEI as N source. Reproduced with permission.[45] Copyright 2019, American Chemical Society.

The atomic-level information of active sites, their molecular geometry, and reaction mechanisms can be identified using operando characterization which allows in situ monitoring of surface oxidation states and local atomic structure transformation.[57–59] In situ measurement can provide real data during the catalytic cycle which promotes the in-depth fundamental understanding of the catalytic system.[60–63]

A large number of wastes and hazardous materials are generated every day and green chemistry can be a sustainable solution to the toxic industrial chemicals. Most of the industrial chemical processes are not highly efficient and produce a large amount of waste, thus increase the atom economy is crucial. How to avoid by-products and achieve 100% atom economy is still an open question as well as highly challenging. Catalyst has been playing a very important role in the chemical industries and to achieve a sustainability goal. A catalyst development using nonexpensive metal which is available in abundance, can only help in increasing the % conversion, selectivity, and lower energy requirements.

Several interesting review articles were published and summarized on various topics.[27,28,64–73] In this short report, we mainly focused on the applications of SACs in benign ways of energy production (ORR, OER, HER, and metal–air batteries), and organic transformations (with and without electrochemical setup) which are published recently.[74–78] Apart from these applications, electrochemical applications of SA for hydrogen electro-oxidation,[79] formic acid,[80–82] methanol,[83,84] and CO oxidation,[85–88] CO_2 transformation into value-added chemicals which is now a day is a hot arena,[74,89,90] N_2 activation,[91–94] and metal–sulfur batteries[95–97] are highly desirable, but discussion about these topics are out of the scope of this report. These topics will be covered separately in the future review article.

2. Role of Single-Atom Catalysts in Sustainable Technologies

Green and sustainable chemistry is a world-shattering philosophy that builds a sustainable society by improving hazardous chemical processes, reduce chemical waste by developing alternative green processes, and reduce the risk of chemical products posed to humans and the environment.[98,99] For the environmentally benign future, there is a need to redesign alternative chemical processes using advanced catalytic technologies because catalysis is a key in the material transformations at the atomic and molecular level. The development of unique highly functionalized heterogeneous metal catalysts based on the cheaply available abundant metal could be an alternate path.[100,101] Preparation of well-defined nanoparticles with controlled size, shapes, and morphologies are used for various heterogeneous catalytic applications.[102,103] The shape control catalysis to define the selectivity and better activity is well known in the heterogeneous catalytic applications of nanomaterials.[104]

The effects of the size of nanoparticles are a much-debated topic in nanocatalysis and are discovered multiple times. It is very important to understand how nanoparticle size played an important role in specific catalytic performance. For example,

Shao et al. discussed the effect of a Pt nanoparticle (in the range of 1–5 nm) on the oxygen reduction in $HClO_4$ solution.[105] It is noted that the ORR activity of Pt nanoparticles depends on the oxygen binding energy, and accessibility of different Pt sites on cubooctahedral particles of various sizes (**Figure 2**a,b). It is well known that the surface reactivity of any particles is associated with surface accessibility, high reactivity of the reactant might block the active sites due to the strong adsorption of intermediates. And low activity might not allow dissociating O—O bond and efficient charge transfer. As shown in Figure 2a, the specific activity of Pt nanoparticles decreased fourfold when the particle size change from 2.2 to 1.3 nm, because surface sites decrease gradually with decreasing particle size while dispersion increase and became maximum for 1 nm nanoparticles (Figure 2a). As the size of the particle decreases, the average oxygen-binding energy of all surface sites is higher than the fcc sites due to contribution from the edge sites (Figure 2b). The presence of edge sites was the main reason for low specific activity which was due to strong oxygen-binding energies on these sites. Both mass activity and specific activity were low for particle size lesser than 2.2 nm. Hence different adsorption sites on the surface of nanoparticles are majorly involved in controlling catalytic activity. However, the shape and size control is now saturated, and there is less possibility for further development.[106] However, the synthesis of shape-controlled nanoparticles with a defined size is highly challenging and tedious. Not only the size and shape, but many other factors including chemical composition, type of support, metal–support interaction, metal and support interaction with the reactant, product, intermediate, and solvent can also have a significant effect on the overall catalytic outcome.[107,108] Recently, the supported SACs catalytic activities have been improved drastically which is equal or greater than the organometallic catalysts.[109] Lately, technology development and characterization techniques have enabled us to prepare a catalyst on a large scale with precisely controlled SA homogeneously dispersed on the support.[110]

At the atomic level, selectivity and reaction conversion can be changed via precisely controlling the atomic cluster or SA.[113] Thus, an SA may show the limited geometric transformation, depending on the type of support. When an SA is stabilized via a functional group, geometry may evolve due to the interaction with the different components of reaction species, and eventually, come into the SA organometallic region.[114] On the other hand, as the cluster size increase from an SA to a group of several atoms (atom less than 20), a different geometric structure may evolve due to the overlap of nearby atomic orbitals.[115,116] Interestingly, the geometric structure of these clusters is quite interesting and could change with the reaction conditions, allowing to change the selectivity and activity. Although it is hard to predict experimentally, theoretical calculations could help in categorizing different atom orbitals. For example, calculations predicted that the geometric configuration of Au_3 cluster can change from linear to triangular when the charge changes from Au^{-3} to Au^{+3}.[117] As the particle size increases more than 40 atoms (>1 nm) geometric structures are less sensitive and more stable, exposed atoms at facet, cornet, or edges; and metal–support interactions changed, etc.[118]
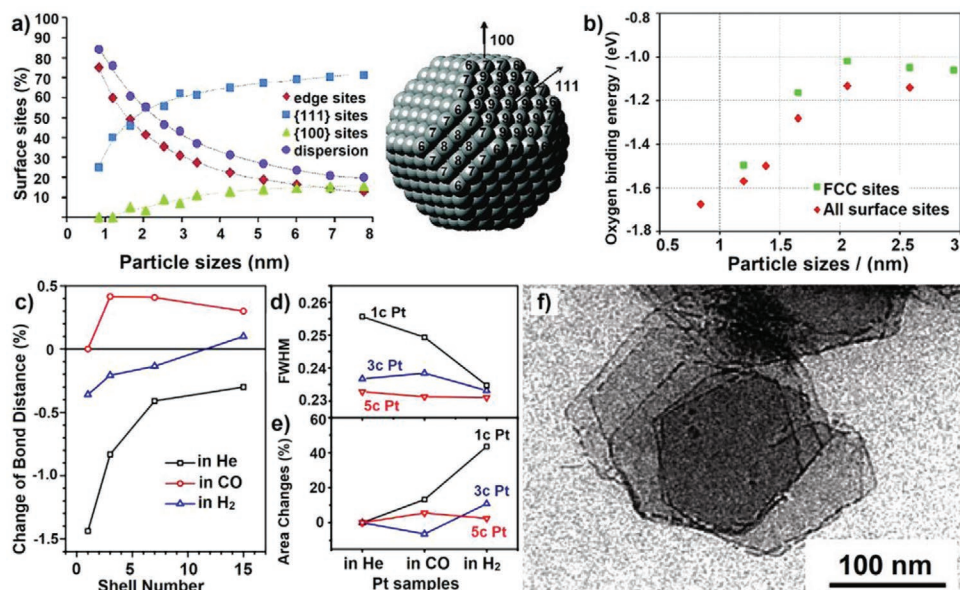
Figure 2. Functions of particle size and shape. a) Size-dependent dispersion and surface percentage of atoms, b) average oxygen binding energy as a function of particle size. Reproduced with permission.[105] Copyright 2011, American Chemical Society. c) Pt–Pt bond distance expansion, d) full width at half maxima, e) area of first Pt–Pt peak at 2.78 Å expansion and contraction obtained from d-PDFs. Reproduced with permission.[111] Copyright 2014, American Chemical Society. f) Porous Pd hexagonal nanosheets synthesized by the reaction of CO with a Pd complex. Reproduced with permission.[112] Copyright 2009, American Chemical Society.

Geometrical deformation also depends on the adsorption of small gas molecules on the metal species. For example, Lei et al. studied the structural changes in Pt nanoparticles (1–3 nm) using CO and H_2 adsorption.[111] A significant change in the Pt—Pt bond was observed when H_2 and CO were adsorbed on the surface of Pt nanoparticles, which was due to orbital hybridization between the metal and gas molecular orbital (Figure 2c–e). This is also the reason for the formation of Pd 2D nanosheets due to the selective adsorption of CO on the Pd surface (Figure 2f).[112] Possibly, CO could replace dibenzylideneacetone (DBA) ligand in $Pd_2(DBA)_3$ and formed an unstable Pd–CO complex which leading to form metallic Pd clusters. These clusters arranged themself into Pd nanosheets on the interface of cetyltrimethylammonium bromide (CTAB). The replacement of DBA ligands by CO was later confirmed by the free energy calculations. The slow diffusion of CO in the emulsion followed by slow reduction and ligand replacement by CO, complexation, or adsorption of CTAB were the key factors for the formation of Pd nanosheets. Hence, molecular interactions are very important phenomena to change the catalytic pathways to tune adsorption behaviors of any species.

Recently, considerable attention has been paid to the developing a variety of methods for a large-scale synthesis of SACs which is only possible by the advancement in the characterization techniques and advanced sustainable methodology.[119] For example, Yang et al. produced Kg scale (transition metal) TM-SACs including Cr, Mn, Fe, Co, Ni, Cu, Zn, Ru, and Pt by the ligand-mediated method with high metal loading.[40] In another report, the electrochemical route has been employed for the production of SACs with high purity and high metal loading.[120] The described method has been demonstrated for the synthesis of Pd, Pt, and Ni SACs anchored on the N-doped

graphene and Fe_2O_3. The advantages of SACs are summarized in **Figure 3**.[121]

3. Single-Atom Catalyst for Sustainable Energy Production

Energy demand is continuously increasing due to the increasing population and globalization. The use of biomass and coal for energy production harms the environment and continuously decreases the quality of air.[122] To tackle these issues, environmentally friendly, renewable-based, clean, efficient energy conversion and storage devices are highly desired. The use of an electrocatalytic setup such as a fuel cell can be an additional unit besides air, solar, and water energy productions. In recent years, a fuel cell has been continuously gaining popularity and has become the frontline research topic as an alternative energy production devices.[123,124] In this section, we are highlighting the use of economical and abundantly available SACs for energy applications. In this section, we are highlighting the use of SACs for various electrochemical reactions and organic transformation.

3.1. ORR

ORR has been extensively researched and has become a major contributor to energy devices.[125] ORR is the most important cathodic reaction in electrocatalysis and among all noble metal-based catalysts such as Pt is the best catalyst for ORR.[126,127] A major limitation of Pt is its high cost, decrease availability for large-scale application of fuel cells. However, dependency
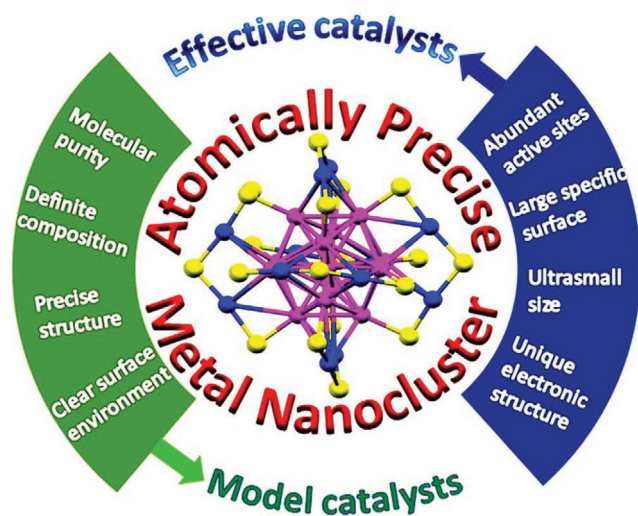
Figure 3. Advantages of SACs. Reproduced with permission.[121] Copyright 2020, American Chemical Society.

on the metal part can be reduced via developing a catalyst with minimal use of metal, keeping in mind not compromise with the electrocatalytic activities.[27] This can be achieved by designing SACs using various support.[128] The development of highly efficient electrocatalyst at low cost is critical for the wide application of sustainable and renewable energy conversion technologies.[73] SACs have attracted significant attention due to their high catalytic activity, stability, and selectivity. Recently, heteroatom-free defected carbon host to anchor Pt-SA for ORR applications have been reported.[129] Pt-SA was stabilized by four carbon atoms in carbon deviancies (Pt–C_4 sites), which were the active sites for ORR. Pt_1/C as a cathode performed a maximum power density of 520 mW cm^{-2} at 80 °C in an acidic H_2/O_2 single cell. Later, an important role of heteroatom doping on catalytic activity, and selectivity have been predicted and proved experimentally. M–N_4 sites, which are responsible for the important behavioral change of SA, are theoretically and experimentally predicted.[66,130,131] In another study Liu et al. reported that pyridinic nitrogen atom anchored single Pt atoms are highly active for the ORR reaction and tolerance to CO and methanol poisoning.[132] Zeng et al. prepared a Pt-SACs grafted on Fe–N_2 centers.[133] The SACs with 2.1 wt% optimum loading exhibited a half-wave potential of 0.80 V compared to Fe–N–C (0.79 V). The enhanced multifunctional electrochemical activity was associated with the Pt–O_2–Fe–N_4 sites, which protected the Fe sites from the harmful deactivating species.[133]

ORR is proceeding with two or four-electron pathways depending on the surface-active sites.[134] Conventional Pt nanoparticles normally followed 4e$^-$ pathways; however, an isolated Pt may not be able to break the oxygen bond due to the absence of adjacent active sites, and the reaction may follow two-electron pathways to produce H_2O_2. Hence by adjusting the distance of the active site, sustainable H_2O_2 production can take place using ORR reaction pathways. Yang et al. produced a Pt-SA supported on titanium nitride (TiN) and SA was stabilized on N-vacancy.[135] The catalyst was used for the H_2O_2 production in ORR, and also used for formic acid, and methanol oxidation.

The Pt/TiN catalyst with 0.35% loading exhibited H_2O_2 production with a high mass activity of 78 A per gram Pt at an overpotential of 0.05 V. However, the H_2O_2 selectivity (more than 90%) for 0.05 and 0.1 wt% Pt/TiN samples were higher than the 0.035 wt% Pt/TiN catalyst. The support also played an important role in catalytic properties similar to the ligand effect in a homogeneous catalyst. The Pt/TiC performed better in terms of catalytic activity, selectivity, and stability for the H_2O_2 production than the Pt/TiN.[136] The better catalytic activity of Pt/TiC might be due to the weak interaction with O_2 molecules which could be the surface poisoning in the case of Pt/TiN. The Pt/TiC did not allow two-electrons pathways which is a major requirement for H_2O_2 production. The chemical nature of support changes the catalytic properties of SA and the dimension of support also significantly affects the outcome of the catalytic reaction. H_2O_2 is one of the most widely used chemicals which can be produced by selective reduction of O_2 to H_2O_2.[137] For selective reduction of O_2, the distance between Pt atoms were adjusted on hollow CuS_x support.[137] The strong interaction between Pt and S (i.e., CuS_x) avoids the formation of Pt–Pt bond which results in individual Pt sites with the ultrahigh loading of 24.8 wt%. Pt/CuS_x can reduce O_2 to H_2O_2 with 92–96% selectivity in a wide range of potential of 0.05–0.7 V in acidic electrolyte. Pt/CuS_x catalyst shows the mass activity of 35 ± 4 A mg_{cat}^{-1} at 0.4 V.

Recently, a study theoretically projected the ORR activity of Ni, Pd, Pt, Cu, Ag, and Au supported on a 2D boron deficient boron nitride (BN) nanosheet.[138] It was observed that d-valence electrons of a metal atom help in the 4e$^-$ reaction pathway and only with the optimized binding strength of OH* species exhibited higher ORR activity. The Pd/BN showed a 0.42 eV reaction barrier compared to the Pt/BN catalyst (0.79 eV). The high catalytic activity is attributed to the formation of M–N_3 coordination sites which is in correlation with the previous studies.[139] Although, the predictions of M–N_x active sites are highly complex and challenging which is hard to control during synthesis.[125] Most of the reports have been discussed the existence of only one type of active site which may be contradicting. However, the existing framework of characterization techniques may not include differentiating differentiation of the actives sites, and the possibility of invisible active sites may not be overruled.[61,140] Note to worthy, recently, Huang et al. reported a synthesis of Fe–N_5 active sites through mimicking the enzyme active centers; Fe–N_5 active sites resembled the heme of natural redox enzyme, i.e., cytochrome P450.[141]

In a similar direction of exploring 2D support, an ultrathin FePt nanosheet was used for anchoring Pt single sites.[142] The SACs were prepared with a high loading of 6.7 wt% Pt with a high electrochemical active surface area of 545.5 m^2 g_{Pt}^{-1} and seven times higher mass activity compared to the commercially available Pt/C catalyst. From a catalysis point of view, bimetallic or nanocomposite of many metals has always some synergistic effect. This could be the reason for the excellent performance of ORR. In this context, Zhang et al. have prepared Pt/Pd single atom alloy (SAA) supported on nitrogen-doped carbon nanotubes using the atomic layer deposition technique.[143] An SA on Pd octahedron exhibited a higher unoccupied 5d-orbital character density of state and a lower

Pt–Pt coordination number. Moreover, due to the atomic dispersion of highly active species in more inert and catalytically selective host metal support, SACs have proven to catalyze a series of electrochemical, photo-electrochemical and thermal industrial reactions.[144,145]

A Pt-based electrocatalyst has been considered the benchmark for electrocatalytic application, however, high cost and low abundance hindered its commercialization on a large-scale production. Therefore, great efforts have been placed in the development of a low-cost catalyst by using earth-abundant materials to replace Pt-based electrocatalysts.[146] In this regard, several abundantly available and low-cost transition metal (TM)-based electrocatalysts such as Cr,[147] Mn,[148] Fe,[149] Co,[150] Ni,[151] Cu,[152] Zn,[153] and Ru[154] have been developed. Apart from the several SA catalysts, the Fe-SA-based one being more explored than the other TM-based catalysts. Several reports predicted the formation of $Fe-N_x$ active sites which were found stable against recyclability, CO, and methanol tolerance.[42] Apart from these studies, $Fe-N_x$ actives sites are also found stable against poisoning agents such as SCN^{-1}. Several methods have been reported for the molecular-level design of Fe-SACs, and, as per rational design, Fe-containing precursors at the molecular level to stabilize the Fe atoms during the high-temperature synthesis. For example, a Fe-electrocatalyst has been prepared via thermal melting of a zeolitic imidazolate metal–organic framework (ZIF-8).[155] For the synthesis of Fe-electrocatalyst, the ZIF-8 was thermally melted with graphene nanosheets and decomposed to generate a thin and active porous carbon layer during the pyrolysis. Such an electrocatalyst possessed a high specific surface area of >1000 m^2 g^{-1} and high catalyst ORR activity with half-wave potential of 0.903 V in alkaline media and 0.837 V in acidic media compared to the commercial Pt/C catalyst. In the same way, ZIF-8 with ferrocene was employed as a molecular precursor of Fe for the preparation of Fe-SA embedded in nitrogen-doped carbon. Molecules of ferrocene already have a Fe-SA at the center and their immobilization on a porous carbon support help to synthesize efficient SACs with high loading and efficient ORR activity. Such a catalyst exhibited a half-wave potential of 0.904 V compared to Pt/C (0.837 V), which is 67 mV higher than the best commercially available catalyst.[156]

It has been theoretically and experimentally proving that the coordination environment has a significant effect on the catalytic properties of metal centers.[157,158] Previous studies demonstrated that $M-N_x$ sites are desired for the excellent catalytic activity of SACs.[159,160] In the case of Fe-SACs, $Fe-N_4$ sites are widely reported as active sites,[161–163] however, it could be possible that $M-N_2$ or $M-N_3$ may also coexist, which cannot be detected spectroscopically. It has been theoretically proven that $Fe-N_2$ sites could be more active than $Fe-N_4$ sites however it is hard to control the types of active sites during the catalyst preparation.[164] DFT calculation predicted that $Fe-N_2$ sites were better than $Fe-N_4$, due to lower interaction with $*O_2$ and OH intermediate and enhance the electron transport. Zhu et al. prepared a bimodal template-based synthesis of $Fe-N_2$ active sites containing SACs.[43] In addition to a decent ORR activity with a half-wave potential of 0.927 V in an alkaline medium, the catalyst possessed high antipoisoning power and a high affinity for O_2. DFT calculation also predicted that the $Fe-N_2$ sites are more

active than the $Co-N_2$ sites for ORR reaction which could be due to the lower energy barrier of the intermediates and products involved. Further, $Fe-N_2$ facilitates the rate-limiting release of OH* and antipoisoning abilities toward SCN^-. Likewise, other researchers also developed a Fe-SA ORR catalyst using graphene for high-temperature polymer electrolyte membrane fuel cells.[165] Many other carbon variants were also used for the preparation of SACs, for example, N-doped carbon nanotube-lined to hollow carbon nanosphere[44] and hierarchical porous carbon[166] have been used for Fe-SA ORR catalyst preparation.

As we have noted, different coordination environments ($M-N_4$, MN_3, or $M-N_2$) have a significant effect on the catalytic properties of SA. Besides this, in combination with N, and other heteroatoms such as S or P can also improve the catalytic activity.[167] Zhang et al. prepared Fe-SACs using an N and S doped porous carbon host (**Figure 4**a–d).[168] FeN_4S_2 have also shown high tolerance to methanol and high recyclability up to 5000 cycles. The DFT modeling predicted that the FeN_4S_2 sites were more active than the CoN_2S_1 and NiN_2S_1 sites (Figure 4), which was due to the higher charge density, the lower energy barrier of intermediate, and the product formed during catalytic cycles. The charge density of metal atom is highly important for ORR activity, and DFT calculation predicted that FeN_4S_2 is 0.11 which is higher than the CoN_3S_1 (0.09) and NiN_3S_2 (0.03), respectively. Figure 4e displayed that the Fe-SA/NSC has the highest density states near to the fermi level compared to Ni and Co-SA/NSC. This Fe-SA/NSC has better electrotransfer properties which are essential for higher conductivity and catalytic performance. The project density of the state (PDOS) of all three metal centers was calculated and particularly, the Fe d-orbitals exhibit higher occupied states near the Fermi level (Figure 4f). For further atomic level information about the good ORR activity, Gibbs free energy (Figure 4g,h) calculation predicted that most endothermic step for CO and Ni-SA/NSC is the last step to form $4OH^-$ with a limiting barrier of 1.15 and 2.79 eV, respectively (Figure 4h). However, the rate-determining step for Fe-SA/NSC demonstrates the different pathways at the formation stage of OH*, and the limiting barrier decrease to as low as −0.65 eV. In particular, the coordinated S atoms played an important role in lowering the reaction barrier which is essential for a good ORR activity. The optimized ORR catalytic activity of Fe-SA/NSC is due to the lower energy barrier of intermediates and methanol tolerance, and also unveiled stability with negligible changes within 5000 cycles.

Not only neighboring heteroatoms are important for tunning the catalytic activity of SA, a neighboring different metal SA may also change essential properties. For example, Sun and co-workers have revealed the active sites and catalytic mechanism of N-coordinated Fe and Ni dual SA-doped carbon for ORR applications.[169] From DFT calculations it was predicted that $FeNi-N_6$ with type-I (each metal atom coordinated with four nitrogen atoms) have better ORR activity compared to type-II, i.e., $FeNi-N_6$ (where each metal atom coordinated with three nitrogen atom. DFT also revealed that different active sites having different ORR activity and activity trends were $FeNi-N_6$ (type-I) > $FeNi-N_6$ (type-II) > $Fe-N_4$ > Fe_2-N_6. As we know that to break the O=O, two adjacent sites are required, and the multimetal-atom structure motif permits the formation of −O−O− bridge model which favors $4e^-$ reaction in an acidic medium.
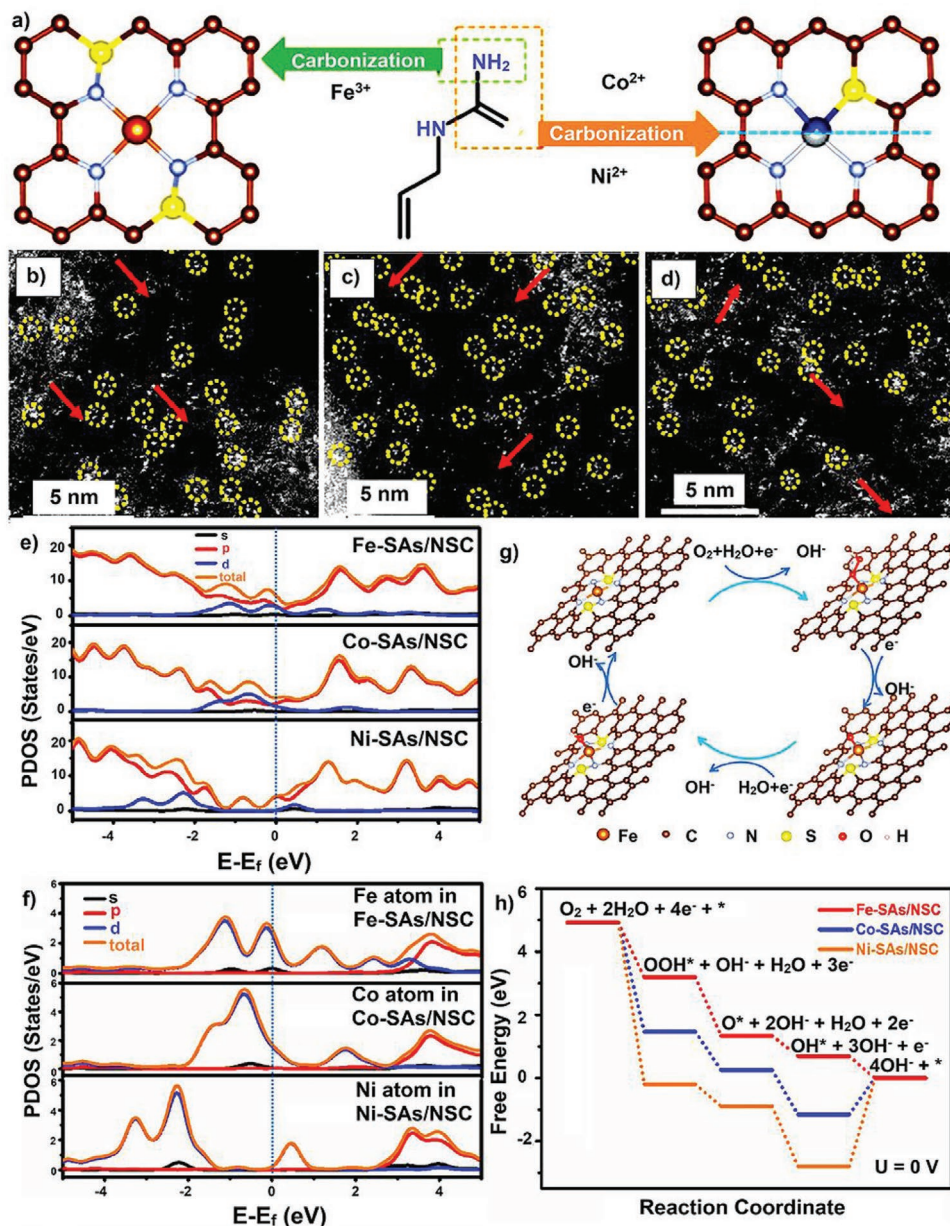
Figure 4. a) Schematic representation of Fe-SA/NSC, Co-SA/NSC, Ni-SA/NSC formation. b–d) HAADF-TEM images of Fe-SA/NSC, Co-SA/NSC, and Ni-SA/NSC. e–h) DFT calculation, (e,f) PDOS of Fe-SA/NSC, Co-SA/NSC, and Ni-SA/NSC, (g) reaction scheme with the intermediates in the ORR process, (h) free energy path of intermediates in ORR on Fe-SA/NSC, Co-SA/NSC, and Ni-SA/NSC. Reproduced with permission.[168] Copyright 2019, American Chemical Society.

The existence of Fe(OH)N$_4$ (half-wave potential 0.88 V) as active catalytic sites was also proved by Zhou and co-workers.[170]

Fe−N$_x$ SACs exhibited the most promising electrochemical catalytic activity, however, it had a serious stability issue due to oxidative corrosion through the Fenton reaction. Fe active sites catalyzed the formation of highly active reactive oxygen species from the reaction with intermediate H$_2$O$_2$ and attacked the carbon substrate which resulted in the degradation of the catalytic activity.[171] This opened a great opportunity for the researchers to solve this issue by developing other metal-based SACs.[172] Luo et al. developed chromium (Cr)−N$_4$ sites for ORR catalytic activity in an acidic medium.[147] Cr−N$_4$ catalyst exhibits

a half-wave potential of 0.773 V and interestingly, Fenton reaction is substantially reduced (checked by the 2,20-azinobis-(3-ethylbenzthiazoline-6-sulfonate) and possesses high stability. Several other Co-based SACs have been reported to tune the electrocatalytic properties of metal centers to develop efficient catalysts.[173–175]

Cu is also a natural choice of catalyst from biology to biochemical to organic transformation.[2,176] Cu can be a good choice for electrocatalytic applications.[176] Recently, the upright ORR activity of Cu was attributed to high redox potential and d-orbital electron density which resulted in the weakening of O−O bonds.[177] Apart from the other application of Cu-based

catalysts, very few reports on Cu-SACs were reported.[178–180] Cu-based SACs prepared via a single pyrolysis method of Cu phthalocyanine as a precursor for the ORR application.[152] The catalyst showed a half-wave potential of 0.81 V in the alkaline medium which was 30 mV lower compared to the Pt/C catalyst. The catalyst Cu-SA/N–C also showed stability up to 5000 redox cycles with only 9 mV negative shift in half-wave potential. Also, the reason for good ORR activity was predicted using DFT modeling and calculation suggested that the process from OOH* to O* is a rate determining step. A simple and scalable approach for the synthesis of SACs was demonstrated via direct transformation of bulk atom to SA and subsequent coordinate with the N-rich carbon.[179] Majority of the SACs were reported the existence of M–N_x active sites in different proportions. In a similar fashion, ZnN_x/C was prepared and atomic dispersion of Zn exhibited catalytic activity similar to that of the other metal.[153,181]

Pt, Pd, and Rh are catalytically highly active phases and components of many commercial catalysts for various applications. Although, the neighboring transition element Ir has rarely been explored for electrocatalytic applications. Xiao et al. have reported Ir-SA supported on nitrogen-doped porous carbon network.[182] ORR activity with TON of 24, $3e^-$ site^{-1} s^{-1} at 0.85 V, and good mass activity of 12.2 A mg$^{-1}_{Ir}$ were reported, which was much better than the commercial Pt/C (Pt 20 wt%) catalyst. The ORR was theoretically modeled the formation of Ir–N_4 sites, and modular adsorption energy of reaction intermediate on the mononuclear Ir–N_4 sites. The optimum adsorption energy of intermediates results in good outcomes. Zhang et al. investigated the ORR activity of SA niobium (Nb) supported on the graphitic layers.[183] Theoretical calculation in resonance with the experimental data Interpretation that graphitic layers produce a redistribution of d-band electrons and become an activist for O_2 adsorption and dissociation and also exhibit high stability.

3.2. OER

Energy conversion technologies based on renewable energy sources such as water, wind, solar, and tidal are a promising way for a sustainable and green pollution-free future. The core of these technologies is electrochemical redox reactions and the implementation of a cheap and largely available metal as a catalyst may push back the frontiers. The OER reaction is a bottleneck of the overall reaction for water splitting and half-reaction can be described as ($2H_2O = O_2 + 4H^+ + e^-$).[184] The reaction consists of four consecutive intermediate steps, which are controlled by many intermediates and active surface sites;[185] several reaction mechanisms using metal centers as an active site have been proposed.[186,187] The OER is a kinetically sluggish anodic reaction and requires a large overpotential to deliver considerable current. Typically, RuO_2 and IrO_2 are candidates for the state-of-the-art electrocatalyst for OER, although they are expensive and serious dissolution during long-term use are their main limitations.[188,189] However, engineering catalytic active sites at the atomic level has become the potential choice to maximize efficiency. Pt, Pd, and Rh based electrocatalysts have appeared also as OER electrocatalysts, although,

efficiency for OER based on noble metal electrocatalyst is far from satisfactory.[190] Finding new materials with higher OER activity and stability is challenging but mandatory. Modification of stable support by anchoring metal SA could be a promising option.[191] This may enable us to tune the electronic structure and binding or interaction with the intermediates and conductivity of the catalytic materials. The fundamental understanding of the active sites and mechanisms using in situ and, even better, operando techniques and DFT calculations are the bases for atomic-level knowledge, and with perspective information can help in tuning the electrochemical activity and efficiency of the catalyst.[53,192–195]

Understanding of thermal stability, microenvironment around the metal centers, and reaction mechanisms are fundamentally desired for its future applications.[196,197] For example, recently, operando XAS and diffusion reflectance infrared spectroscopy in combination with mass spectroscopy was utilized to understand the Pt dispersion, oxidation states, and CO oxidation activity.[198] Notably, Pt-SA (Pt^{m+} atoms where m ≥ 2) gradually converted into highly active ≈1 nm size Pt$^{\delta+}$ clusters ($\delta < 2$). The dynamics of SA was predicted, might high oxidative conditions and high temperature leads to the formation of bigger particles with the low catalytic activity.

M–N_4 sites are majorly proposed as electrocatalytic active sites for the ORR, these single atomic sites could be highly active for the OER. Cao et al. reported the synthesis of Ru–N_4 sites supported on an N-doped porous carbon.[154] The electrocatalyst exhibited high activity and reached mass activity as high as 3571 A g$_{metal}^{-1}$ and TON of 3348 O_2 h^{-1} at a low overpotential of 267 mV at a current density of 10 mA cm^{-2}. The DFT calculations indicate that the first activation step involved adsorption of a single oxygen atom on a Ru site to form O–Ru_1–N_4 which reacted with water through the nucleophilic attack followed by deprotonation to generate OOH*. The O–Ru_1–N_4 increases the valence state of Ru with more oxidation states which are the active sites for OER. Hence, the O–Ru_1–N_4 has a lower barrier of O–O coupling to form OOH* intermediate.

A scalable nanocasting approach was recently reported for Pt-SA decorated porous NiO and SiO_2 was utilized as a hard template.[199] Bulk Pt-doped NiO nanocubes were prepared by impregnation, drying, calcination in air, and SiO_2 was removed using NaOH. A large scale, around 200 g of 0.5 wt% Pt/NiO nanocubes was prepared in a single batch using a nanocoating approach, as well, other variants using ALD and impregnation were also prepared for compression using an impregnation method. The OER activity order was 0.5 wt% Pt/NiO > ALD-Pt/NiO > 1 wt% Pt/NiO > NiO. The first-principles calculation indicated the charge transfer from Pt to Ni through O leads to a local weaker Ni–O bond.[199] The Pt helped in an effective phase transformation from NiO to γ-NiOOH rate by reducing the migration barrier of the nearby Ni atom. The phase transition of NiO to γ-NiOOH in alkaline medium was an origin of OER activity and the thickness of γ-NiOOH phase was estimated, i.e., 0.5 wt% Pt/NiO > ALD-Pt/NiO > NiO which was in agreement with the OER activity.[199]

Boosting the OER of single atomic sites using electronic coupling with layered double hydroxide (LDH) could be another way.[200] Ru-SA decorated Co/Fe double hydroxide comprises a strong electronic coupling between Ru and a layered double
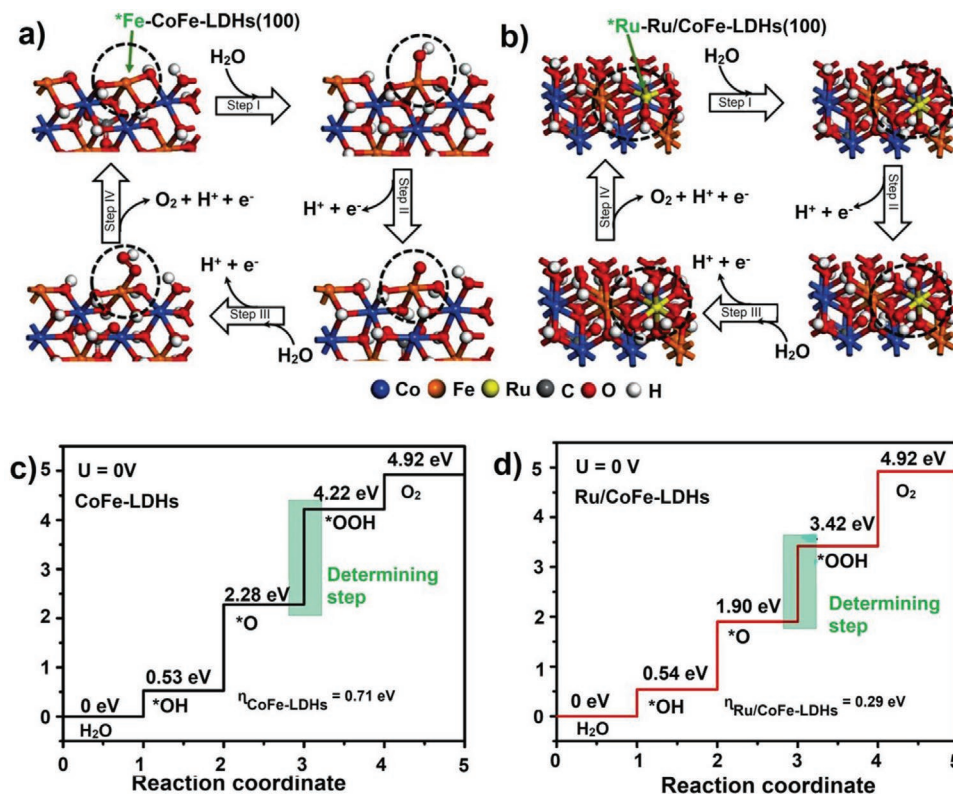
Figure 5. Theoretical OER overpotential for CoFe-LDH and Ru/CoFe-LDH, a) Proposed four electrons mechanism of OER on CoFe-LDH, b) for Ru/CoFe-LDH. Gibbs free-energy diagram for four steps of c) OER on CoFe-LDH and d) Ru/CoFe-LDH. Reproduced with permission.[200] Copyright 2019, Nature Publishing Group.

hydroxide. A Ru/FeCo-LDH exhibited high electrocatalytic activity with an overpotential of 198 mV at the current density of 10 mA cm^{-2} and a small Tafel slope of 39 mV dec^{-1}. Spectroscopy measurements revealed that Ru remains in the (IV) oxidation state even at high overpotential due to the synergistic electron coupling with Fe and Co.[200] The first-principles DFT simulations and Hubbard U (DFT + U) calculations have been used to stimulate the OER process based on the 4e$^-$ mechanism. The Ru/FeCo-LDH was considered as loading ruthenium hydroxide complex on 001 crystal plane of LDH by releasing one water molecule and Ru atom coordinated with five oxygen atoms which increased the oxidation states. The optimized structure of intermediates is presented in **Figure 5**a,b. For CoFe-LDH and Ru/FeCo-LDH, the formation of *OOH group from *O was found to be the rate-determining step (Figure 5c,d). For the rate-determining step, Ru-SA on the surface of CoFe-LDH showed the lowest Gibbs free energy (1.52 eV) than the Fe-SA on the edge of FeCo-LDH (1.94 eV). The strong electronic coupling interaction between Ru and CoFe-LDH surface tuned the electronic and coordination state or Ru-SA which allowed Ru atom to exist in a lower +4 oxidation state. Engineering single atomic sites on the surface of LDH provide better stability and catalytic activity, for example, Chen et al.[201] developed Ir-NiFe-LDH; and Feng and co-workers[202] synthesized Ru-NiFe-LDH. Zhang et al. used Au-SA decorated NiFe-LDH for OER applications, 0.4 wt% Au loaded NiFe-LDH exhibited sixfold OER activity enhancement.[203]

Electrochemical deposition is a universal route for the fabrication of SA electrocatalysts.[204] Lai et al. used a general p-electron assisted strategy for Ir, Pt, Ru, Pd, Fe, and Ni SA electrocatalyst preparation.[205] Metal atoms can be simultaneously anchored on two different domains—NC$_3$ and centers of Co octahedra of hybrid support. Two distinct SA metal sites worked as a bifunctional electrocatalyst for both OER and HER. The Ir-based bifunctional electrocatalyst outperformed all the other metallic sites and DFT calculations showed that Ir@Co sites can accelerate OER and Ir@NC$_3$ sites are responsible for HER.

The TM-based electrocatalyst is emerging as a promising OER catalyst and may fulfill our vision of a sustainable and green society. Several reports on the use of metal oxides and SA decorated metal oxides were reported as favorable OER electrocatalysts.[206–209] However, to push its electrochemical activity further, it is necessary to understand the relation between the structural and its properties by precise control of composition or loading, synergy with other neighboring metal centers, or support or cooperativity and reaction media.[210–214] Fei et al. presented a general synthesis for SACs and also identified the molecular structure of the active sites.[215] For the electrocatalyst preparation, N-doped graphene was utilized and metals including Fe, Co, and Ni were used to demonstrate the efficacy of the synthesis process. The size-dependent electronic structure and the catalytic activity suggest that the atomic metal could have different catalytic behaviors. The electrocatalytic properties can be tuned by the ligand-field effect which may

differ depending on the metal center and molecular coordination configuration with N and C. The possibility of occurrence of MN_4C_4 sites was expected because the C atoms close to N and these should have preferentially binding sites for oxygen intermediates than the N itself, which is due to doping induced charge redistribution. Based on the effect of the metal center, electronic environment, and energies of different intermediate, the OER trend was Ni > Co > Fe. The $Ni–N_4C_4$ electrocatalyst may be further enhanced by increasing the metal loading and density of active sites. The OER catalytic activity may further improve by using the combination of two or three metallic systems such as bimetallic or SAA. For example, Bai et al. used a combination of a Co and Fe double atom to boost the OER electrocatalytic performance,[216] and several SAA[30,217,218] were also reported for OER applications.

3.3. HER

H_2 is referred to as a fuel of a sustainable future and as an advanced way to decarbonize our environment. Recently, a few countries including Germany have initiated a passenger train based on H_2 as a fuel, Nevertheless, sustainable production of H_2 is remaining a challenge.[219] The H_2 production via HER has been researched as an alternative clean fuel for various uses.[220] In this regard, the H_2O electrolysis in alkaline media is of primary importance because it is the only largely employed technology worldwide and may become a game-changer to achieve a sustainable future.[221] Recently, $Ni_5P_4–Ru$ active sites were found highly active and long term stability for alkaline H_2 production with the low onset potential of 17 mV and an overpotential of 54 mV at a current density of 10 mA cm^{-2} with a Tafel slop of 53 mV decade^{-1}.[222] The development of efficient electrocatalysts is crucial, and a large number of active electrocatalysts for HER in an acidic medium have been reported. However, an acidic medium cause corrosion of cells and contaminates the H_2 gas due to the formation of by-products.[223] Advancement in HER can be further accomplished via developing a heterogeneous or SAC electrocatalyst; and noble metal-based catalysts already proved the dominance in this field.[224–231]

Recently, noble metals (Pt, Pd, and Ir) based electrocatalysts have been the most active materials for HER, although high cost, easy agglomeration, and poor stability in an acidic medium impede their further development.[232] A Pt-SA coordinated with graphdiyne (GDY) has been developed for HER reactions.[233] The GDY formed two types of complexes with a Pt atom, $C_1–Pt–Cl_4$ (Pt-GDY1) created five-coordinated species, and $C_2–Pt–Cl_2$ (Pt-GDY2) form 4-coordinated species. The Pt-GDY1 displayed high catalytic activity for HER with a mass activity of 23.64 A mg^{-1} which was 3.3 and 26.9 times higher than Pt-GDY2 (7.26 A mg^{-1}) and Pt/C (0.88 A mg^{-1}). This was due to the higher total unoccupied density of state of the Pt 5d orbital and close to the zero value of Gibbs free energy of hydrogen production. Similarly, an SA can also be stabilized using carbon vacancies. A series of TM such as Cu, Ag, Au, Ni, Pd, and Pt were immobilized on TiC.[234] Carbon vacancies in TiC helped to stabilize SA and the overpotential for HER versus SHE were 230, 220, and 156 mV at 10 mA cm^{-2} for Au/TiC, Pd/TiC, and Pt/TiC, respectively. Pt/TiC showed 6.5 and 3.5 times higher electrocatalytic activity compared to Pt/C and Pt (NP)/TiC, respectively, which was in consistent with the theoretical calculations. In a similar line, a carbon defect derived Pt atomic cluster (with a precise number of atoms) catalyst was reported for efficient HER.[235] Jiang et al. investigated HER activity of Pt-SA embedded in nonporous cobalt selenide (CoSe).[236] The catalyst exhibited a Tafel slope of 35 mV dec^{-1} and a high turnover frequency of 3.93 s^{-1} at -100 mV in a neutral medium versus RHE, which easily outperformed the commercial Pt/C catalyst.

2D materials including graphene can be good for the electrocatalytic application of SACs.[75,237,238] Sun et al. used N-doped graphene for the preparation of Pt-ACCs (atomic cluster catalysts).[239] The Pt-NG/C exhibited a higher catalytic activity than the single atomic counterpart after 4000 cycles and more than 16 h HER reaction in an acidic medium. Apart from N-doped graphene, N-doped porous carbon is also a good support for the preparation of SACs. A titanium carbide ($Ti_3C_2T_x$) MXene which is a newly discovered 2D material was also employed for the preparation of Ru-SACs.[240] For coordination, S and N heteroatoms were utilized and $Ru–N/S–Ti_3C_2T_x$ electrocatalyst exhibited a current density of 10 mA cm^{-2} at a low potential of 76 mV. Apart from this, $Ru–N/S–Ti_3C_2T_x$ also exhibited superior photoelectrochemical activity with a high photocurrent density of 37.6 mA cm^{-2} which was higher than the Pt and other noble metal-based catalysis coupled with a Si photocathode. Many Ru and Ir-SA-based electrocatalysts were reported for HER outperformed Pt/C catalyst.[241–244] Du and co-workers prepared a silver (Ag) SA electrocatalyst for HER using laser ablation in liquid to generate high density stacking faults in Ag nanoparticles.[245] The stacking faults can cause a low coordination number and high tensile strain which improved the adsorption energy and also transformed nonactive Ag in highly active catalytic sites. Ag-SACs achieved a current density of 485 mA cm^{-2} at −0.3 V, which was 1.7 times higher than Pt/C (282 mA cm^{-2}) and was highly durable for 5000 cycles. All the reported SACs have predicted that SA is the only active site; however, a defect may also contribute to catalytic activity which is hard to differentiate and challenging to measure.[246] Cui et al. introduced Co SA bound to distorted MOS_2 with an ensemble effect for HER.[247] Active-site blocking experiments and DFT calculation revealed that the superior electrocatalytic behaviors are due to the synergistic effect of Co and S of MoS_2.

HER electrocatalytic properties can be further improved by the synergistic effect of two different metallic atoms. In this regard, a combination of Pt–Ru bimetallic dimers were employed to further boost the HER activity, and ALD was utilized to adorn the bimetallic Pt–Ru on the N-doped carbon nanotube (N-CNT) (**Figure 6**a).[248] Cyclic voltammeter of Pt–Ru/NCNT, Pt-SA, and Pt/C were recorded in 0.5 M H_2SO_4 at a scanning rate of 50 mV s^{-1}. Figure 6b shows the HER curves of the different catalysts and the result indicated that the Pt–Ru/NCNT was a much better catalyst compared to Pt/C and Pt-SA. The Pt-Ru/NCNT showed a mass activity of 23.1 A mg^{-1} at the overpotential of 0.05 V which was 54 times greater than that of the Pt/C catalyst (Figure 6c). After accelerated degradation tests (ADTs) Pt–Ru/NCNT catalyst exhibited similar activity like before (Figure 6d) and HER showed of 5% loss of activity at the overpotential of 0.05 V, while the Pt-SA demonstrated 9%
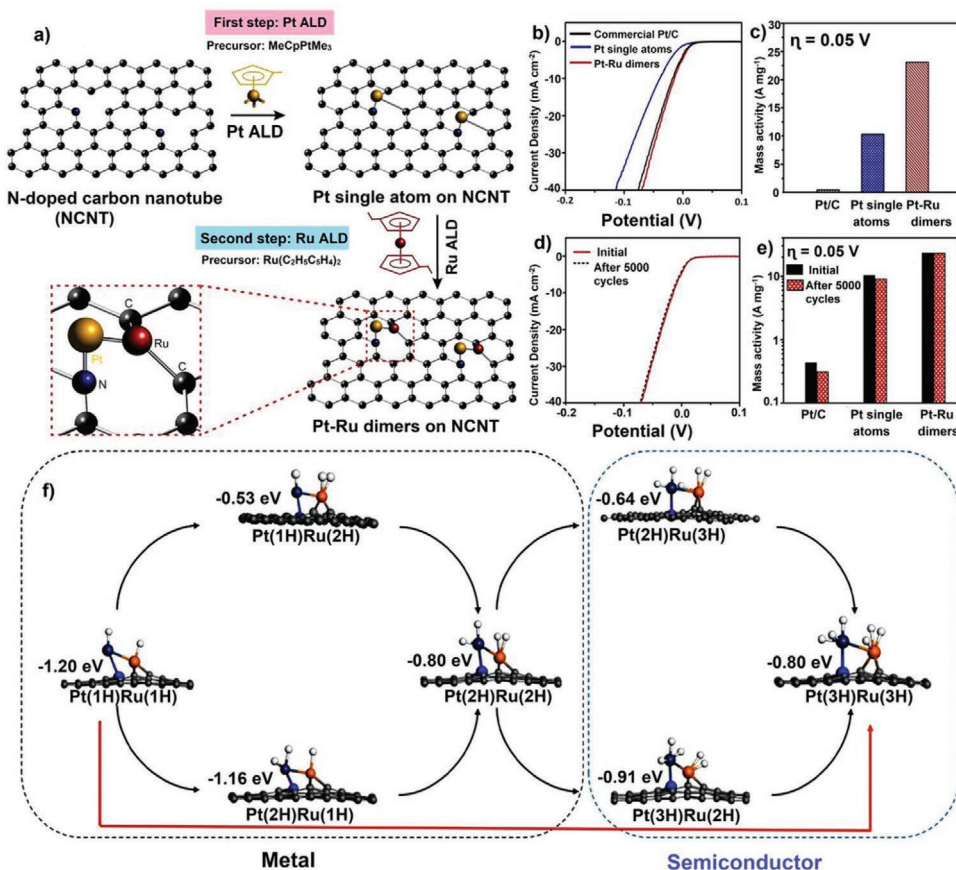
Figure 6. a) Scheme for ALD of Pt-Ru/NCNT. HER electrocatalytic performance of Pt-Ru/NCNT dimer, b) Pt-Ru/NCNT, Pt-SA, Pt/C, c) normalized mass activity at 0.05 V, d) durability test for 5000 cycles, e) normalized mass activity after ADTs. f) H_2 adsorption configuration of Pt–Ru/NCNT. Reproduced with permission.[248] Copyright 2019, Nature Publishing Group.

loss (Figure 6e). On the other hand, the Pt/C exhibited a 28% decrease in the HER activity which was a lot compared to the other two versions (Figure 6e). The TEM analysis was also performed after the ADTs and indicated the existence of a similar dimer Pt–Ru structure. Overall, the Pt–Ru/NCNT shows much higher electrocatalytic activity which is 50 times compared to Pt/C. The DFT energy calculations displayed adsorption energies of Pt–Ru/NCNT and Ru–Ru were −1.3 and −4.87 eV respectively, which indicated that Ru prefers to make Pt–Ru instead of Ru–Ru dimer. The total hydrogen adsorption on active sites was calculated which was gradually increased from 2 to 6, by repeating the sequential adsorption of H atoms; each can hold three atoms (Figure 6f).

Catalysts are the backbone of electrochemical processes and a series of TM-based SA catalysts such as Fe, Co, Ni, and Zn have been reported.[249–252] Lai et al. reported a comprehensive strategy to synthesize a series of the catalyst including TM such as V, Mn, Fe, Co, Ni, Cu, Ge, Mo, Ru, Rh, Pd, Ag, In, Sn, W, Ir, Pt, Pb, and Bi.[253] From all series of variants, Ge, In, Sn, W, Pb, and Bi-based catalysts have a poisonous effect on the HER performance. It has long been predicted that heteroatom doping such as B, N, P, and S can increase electrocatalytic performance due to the synergistic effect between dopant elements and substrates.[254] Out of series of electrocatalysts, Mo/NC, Fe/NC, and Ir/NC showed good activity toward HER with

minimum potential and fast kinetics; Fe/NC exhibited high durability for 5000 cycles. Further, SA Co supported N-doped graphene,[255] and porous carbon[256] were also utilized for HER reactions.

3.4. Zinc–Air Batteries

Large-scale electrical energy storage using rechargeable batteries works toward the current goal to shift fossil fuels to electric energy by deploying renewable sources, batteries are the way to store electric energy and can be used on-demand.[257] Many variants of batteries are produced such as Li–S, Na–S, or metal–air.[253,258–260] Metal–air batteries (MABs) hold high energy density and a potential candidate for the future energy supplier of the next generation.[261] MAB is generally composed of a porous cathode, electrolyte, and metal anode. The selective interaction with O_2 at the cathode is highly desirable for the high performance of MAB; and other components such as CO_2 and H_2O can also react with the metal anode which results in a decrease of overall battery performance.[262] Bifunctional electrocatalysts of ORR and OER are critically important for the development of efficient MAB.[263] An efficient heterogeneous electrocatalyst based on metal-free catalysts such as porous carbon[264] and heteroatoms doped porous carbon,[265]

12

noble metals, and TM were made significant progress, and further development of SACs enhanced the electrocatalytic performance.[266–268] In recent years, increasing interest in higher energy density, cheaper, and safer battery technology has stimulated tremendous research efforts toward the development of improved rechargeable Zn–air batteries (ZAB).[257] ZAB is one of the promising sustainable and green candidates using abundant and inexpensive resources with a decent energy density, and high reduction potential.[269] Number of decent efforts has been invested in for increasing the active sites, accessibility, and selectivity for electrocatalytic materials are effective for improving air electrode performance.[270] The SACs have been reported to exhibit a decent electrocatalytic activity for ORR, OER, and HER, which can be used as a potential air-electrode in ZAB.[97,271,272] For example, Co-SA with CoN_4 active sites supported on N-doped graphitic nanosheet exhibited excellent catalytic activity for ORR, OER, and Zn–air battery.[273] In another example, Co-SA doped porous N-doped carbon exhibited good performance in solid-state Zn–Air battery and showed cycling stability of 125 cycles with an open circuit potential of 1.411 V.[274]

Metal SA doped M–N_x sites are majorly reported and also attract wide attention due to remarkable tuneability, selectivity, high efficiency, and diversity.[71] The coordination between the metal atom and N atoms significantly tunes its electronic environment, which helps to reduce the adsorption energy for intermediates.[275] Although the N coordination has a significant effect on the electronic environment of SA, the electrocatalytic performance may be further tuned with the help of another heteroatom doping such as S, P, B, F, etc. in combination with N doping.[276] In this direction, Xie et al. developed an N and S coordinated Fe-SA electrocatalyst for ZAB by pyrolysis of CNT, 2,2-bipyridine, and Fe precursor under N_2 atmosphere. S, N–Fe/CNT electrocatalyst showed excellent cyclic stability with no change in voltage after 100 cycles.[277] Hence, designing the optimized coordinated catalytic active sites is a promising and sustainable path for designing and preparing a highly efficient catalyst. Han et al. demonstrated a Fe–Nx–C electrocatalyst synthesized by incorporating in situ Fe-Phen complexes into nanocages during the ZIF-8 growth, followed by pyrolysis at 900 °C in an inert atmosphere.[278] Fe–N_x–C cathode showed a high open-circuit voltage of 1.51 V and a high power density of 96.4 mW cm^{-2} with a good recyclable performance for 300 h with an initial round trip efficiency of 59.6%. The overpotential increases from 0.862 to 1.991 V at the last 300th cycle, and round-trip efficiency decrease to 25.8%. After the analysis of the deposited material on the Zn anode, it was found that the Zn was in metallic form. A solid-state battery made of a Fe–N_x–C catalyst exhibited an open-circuit voltage of 1.49 V and long life of 120 h.

To further tune the electronic environment around metal atomic sites, P and S were doped along with N on hollow carbon which was designated as Fe-A/NPS-HC.[279] The polymer-based coating facilitates the construction of a hollow carbon via the Kirkendall effect and the electronic modulation of a Fe center can be manipulated by long-range interaction with S and N (**Figure 7**a) which is visible in TEM images (Figure 7). The Fe-A/NPS-HC based battery exhibited a high open-circuit voltage of 1.45 V compared to Pt/C-based ZAB

(**Figure 8**a), and also achieved a high as 195 mW cm^{-2} with a high current density of 375 mA cm^{-2} (Figure 8b). Both current and power density (177.7 mW cm^{-2} and 283 mA cm^{-2}, respectively) outperformed the Pt/C catalyst.

Rechargeability and cyclic durability of a catalyst are of great significance (Figure 8c), Fe-A/NPS-HC initially showed a charge potential of 2.07 V and a discharge potential of 1.11 V.[279] Lower charge and discharge voltage difference exhibited better rechargeability of Fe-A/NPS-HC. The ZAB indicated a negligible change in voltage after 500 charge–discharge cycle tests with 200 000 s, specifying the outstanding long-term durability of SACs (Figure 8c). Figure 8d shows the polarization and power density curves of proton exchange membrane fuel cells in an acidic medium (PEMFCs) at the testing temperature of 60 °C. Fe-A/NPS-HC in the membrane electrode assembly (MEA) exhibits a noteworthy current density of 50 mA cm^{-2} at 0.8 V, which is comparable to the highest current density of 75 mA cm^{-2} reported so far. The maximum power density of Fe-A/NPS-HC-based MEA was 333 mW cm^{-2} at 0.41 V which was 92% of the power density of Pt/C-based MEA under similar conditions. Yang et al. also produced a Fe-SA catalyst for ZAB, after 200 000 s, 93.6% of the current density at 0.8 V was retained which demonstrated the good durability of ZAB.[280]

Many different strategies have been reported for the synthesis of SACs and numerous porous materials as a precursor were employed for the synthesis. Peng et al. used a covalent organic framework (COF) for the preparation of the Fe-SA catalyst and showed ZAB durability for more than 300 h.[281] Similarly, $FeCl_3$ encapsulated Porphyra precursor pyrolysis strategy was used and porous S-doped Fe–N–C nanosheets were synthesized.[282] The Fe-NSDC electrocatalyst assembled rechargeable ZAB exhibited a higher power density of 225.1 mA cm^{-2}. Fe-NSDC based ZAB also exhibited lower charge–discharge overpotential and high current density (1 V, 100 mA cm^{-2}) compared to Pt/C + RuO_2 catalyst (1.09 V) and Fe-NDC (1.61 V). This could be due to the S-doping optimized charge and spin distribution on Fe-SA to develop good electrocatalytic properties which were ascribed to Fe–N_x and Fe–N_3/S. Apart from the N, S, F doping, P—O bond can also change the intrinsic properties of the metal SA. It was proved theoretically and experimentally that the P—O bond can effectively update the Fe center electrocatalytic properties and also help in the dispersion of the Fe–N_4 sites.[283] The P–O group produced a favorable surface electronic environment and thus, enriched the catalytic activity. The P–O/FeN_4-CNS catalyst exhibited a power density of 232 mW cm^{-2} and a robust cycling performance of 450 cycles under 25 mA cm^{-2}. Additionally, the solid-state ZAB also exhibited a large energy density of 109 mW cm^{-2} and a long lifetime of 20 h.

The Fe–N_4 catalytic sites were developed via the polymerization–pyrolysis–evaporation (PPE) strategy and the obtained Fe-N_4 sites exhibited superior trifunctional electrocatalytic performance for OER, OER, and HER.[284] The Fe–N_4 sites revealed good stability at a current density between 10 and 100 mA cm^{-2} for 23 h and lower power density (232 mW cm^{-2}) than the Pt/C + Ir/C based battery (50 mW cm^{-2}). To prove the novelty of the PPE strategy, a series of TM such as Fe, Co, Ni, and Mn were anchored on a N-doped porous carbon. Bimetallic SA anchored on N-doped hierarchical meso/microporous FeCo–N_x–carbon
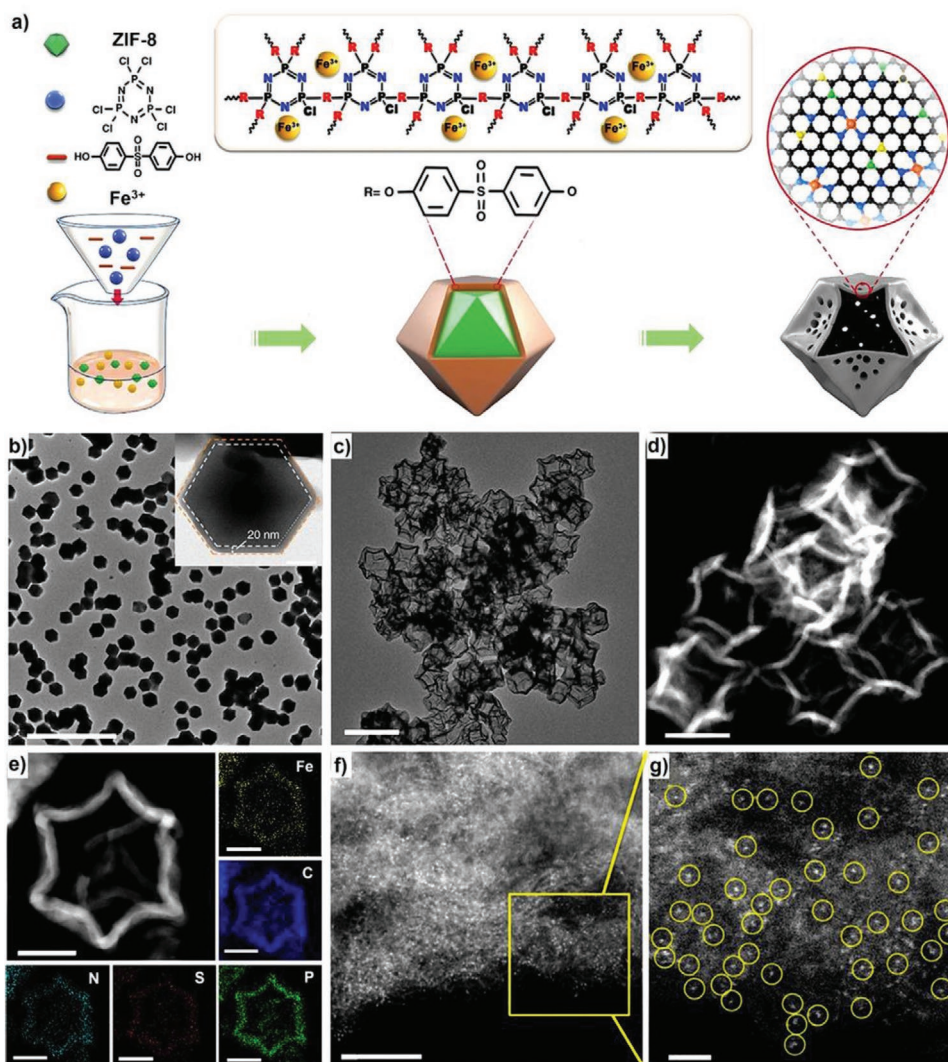
Figure 7. a) Scheme for the synthesis of Fe-A/NPS-HC, b) TEM images of ZIF-8 with precursor coating (scale bar: 2 µm), c) TEM image of Fe-A/NPS-HC (Scale bar: 500 nm). d) High angle annular dark-field scanning TEM images (HAADF-STEM) (scale bar: 200 nm). e) Enlarged HAADF-STEM images and corresponding elemental mapping. f,g) Aberration-corrected (AC) HAADF-STEM images, (f) 5 nm and (g) 1 nm scale bar. Reproduced with permission.[279] Copyright 2018, Nature Publishing Group.

nanosheets were used for ZAB.[285] For the synthesis, silica was used as a template and exhibited a maximum power density of 150 mW cm^{-2}, which was found three times higher than the Pt/C. Rechargeability is a good parameter to look for the stable ZAB battery, and the catalyst was found stable for more than 20 h under 20 mA cm^{-2} with the charging–discharging voltage gap of 0.91 V. The good performance of bimetallic SA electrocatalyst is due to i) the nanometer thickness of carbon sheet can efficiently enhance transport of both electron and oxygen, ii) the combination of Fe and Co with N-doping can modulate electronic properties and surface polarities, iii) the high specific surface area and balanced microporous and mesoporous structure make active sites fully accessible to relevant species and improve the transport properties.

Similar to the Fe–N$_x$ active sites, outstanding electrocatalytic properties, and the durability of ZAB made of Co–N$_x$ were also reported.[274,286–291] In a similar line, superior ZAB performance using a Co-SA supported on the zeolitic imidazole framework was also reported.[291] Furthermore, in another work, binder-free cathode SACs on self-supported porous carbon flake was synthesized via the impregnation–carbonization–acidification strategy.[292] The Co atoms supported on N-doped porous carbon flake employed for wearable ZAB established a satisfactory current density of 6.25 mA cm^{-2}, energy storage capacity of 530.17 mAh g$_{zn}^{-1}$, good rechargeability for 90 cycles, and stability for 900 s. The superior performance of Co SA based binder-free cathode are due to the following reasons i) low catalytic barrier for O$_2$ catalysis, ii) highly accessibility of active sites due to its hierarchical porous network, iii) binder-free design to control active sites and surface morphology of electrode, and iv) high conductivity and good mechanical properties.
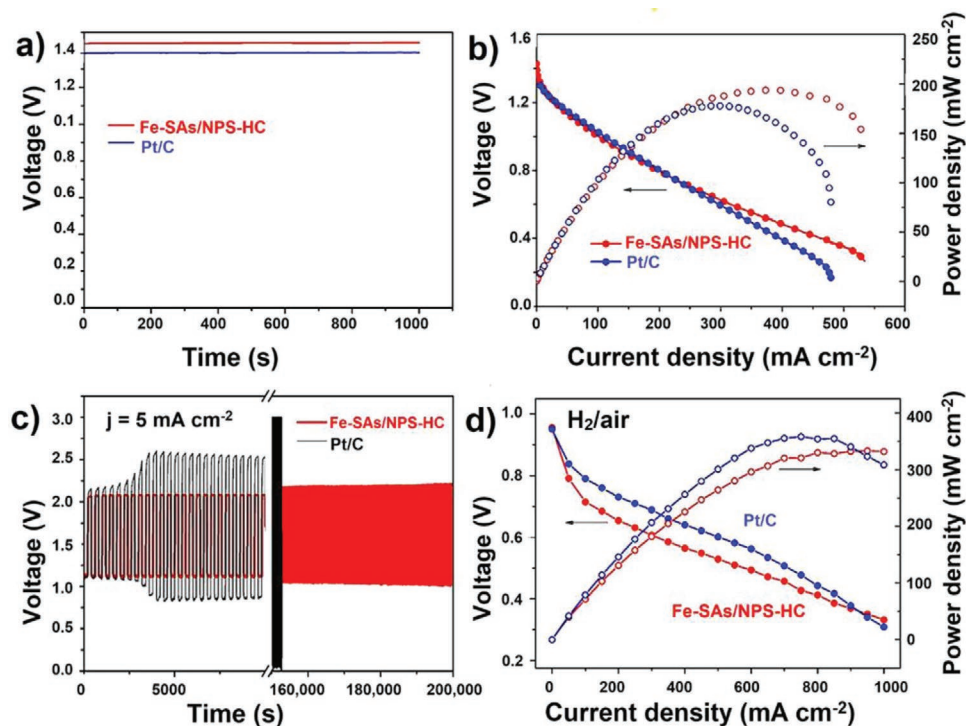
Figure 8. Zinc–air battery performance and hydrogen–air fuel cell performance. a) Open-circuit voltage curve, b) discharge polarization curve, and corresponding power density plots. c) Charge–discharge cyclic performance and d) H_2–air fuel cell polarization curves and power density plots. Reproduced with permission.[279] Copyright 2018, Nature Publishing Group.

3.5. Electrochemical Organic Transformations

The performance and cost of the electrocatalyst play an important role in its development and applications in energy conversion and environmental remediations. The development of synthetic strategies and fundamental understanding at the atomic scale is playing an important role in its advancement. Notably, the electrochemical process produced several electrons and intermediates can be extracted during the process and can be utilized for additional organic transformations.[293–295] The process of carrying out the organic transformation using electrochemistry is known as organic electrochemistry,[296] and by using this energy-efficient technique, a wide variety of important energy extensive organic transformations can be performed.[297] Electrochemical organic transformations (EOTs) can be utilized to minimize waste production, i.e., are more environmentally friendly, reduce the number of steps, allow milder reaction conditions, and provide an alternative path to accessing the desired product.[298] The EOT can perform direct, indirect, or paired electrolysis with other electrochemical processes such as OER, ORR, or HER.[299,300] These strategies for C−H and C−N bond formation using the anodic electrochemical method have been summarized.[301–303] The use of a redox mediator to achieve indirect processes has been significantly increased. Francke et al. reviewed the basic principles and fundamentals of redox catalysis in organic electrosynthesis.[304] Although, extensive works on the use of an electrochemical system for organic transformations are reported, none of them discussed the use of SACs, therefore several metal-free carbon-based organic electrosynthesis have been published.[305–307]

The conventional ways of utilizing SACs for organic transformations have been used and summarized.[308] The use of SACs with electrochemical setup may further revolutionize the yield and better selectivity. Yuan et al. coupled HER with electrochemical oxidative cross-coupling of thiols and thiophenols with arenes, heteroarenes, and alkenes catalyzed by TM.[309] An alternative protocol was developed for halogenation under water-free conditions using methanol, an acetonitrile solvent mixture, and a variety of halogenated reagents such as CBr_4, $CHBr_3$, CCl_3Br, and CCl_4. A wide range of efficient and benign methods have been developed for the direct formation of C−S, C−N, C−Br, C−Cl, C−O, C−P, S−S, and C−C bonds. The undivided organic electrochemical cell was able to achieve >90% yield and Pt electrode helped to transfer the proton from H_2 to the organic molecules. Despite the good achievement in oxidative coupling of organic molecules with the excellent yield for the C−H(sp³) and the C(sp²)−H functionalization, C(sp)−H is highly challenging. In another example, the HER was coupled with an electrochemical oxidative coupling of oxysulfenylation and aminosulfenylation of an alkene.[310] Recently, Jiao et al.[311] and Ackermann et al.[312] also demonstrated the use of TM as a catalyst for C−H functionalization of the C−H bond. Concerning the C−H functionalization, Rh(III) catalyst employed for C(sp)−H functionalization with a high level of regioselectivity and functional group tolerance; and C−C activation respectively.[313,314] Although several reports have been published using an electrochemical setup to demonstrate the use of TM as a homogeneous metal ion catalysts for organic transformations, none of them utilize supported SACs.[315–323] The use of heterogeneous SACs has better advantages than

15

the homogenous and heterogeneous catalyst, mainly, they are abundant active sites, large specific surface, ultrasmall size, and unique electronic structure.

3.6. Organic Transformations

Fine chemicals are an important ingredient of many important industrial applications, however, the manufacturing of fine chemicals via efficient processes, high selectivity, and without harming the environment is challenging.[324] With increasing concern about the environment and contaminating life supportive materials including food, water, and air, there is an urgent need to develop an efficient green and sustainable catalytic process.[325] Till now, several organometallic homogenous SA catalysts have been demonstrated at the industrial level, they are usually sensitive to air and moisture, which are hard to separate at the ppm-level.[326,327] With the rapid development of SACs for various applications in electrocatalysis, the use of SACs for organic transformations are still under development and no explored highly.[328] For example, Pt_1/FeO_x SACs were three times more active than Pt nanoparticles for CO oxidation.[20] The high catalytic activity is due to the presence of active sites at the atomic level and with time, SACs become the leader of heterogeneous catalysis for organic transformation. For example, Pt–Cu SA nanoalloys were used for the hydrogenation of 1,3-butadiene[49] and a Co–N–C SA atom catalyst was employed for the hydrogenative coupling of nitroarenes.[329] CoN_4C_8-1-$2O_2$ active sites coordinated with the four pyridinic N atoms in the graphitic layer were identified as the active sites, and exhibited excellent chemoselective hydrogenation (around 90% conversion in 2 to 7 h, depending on reactant used) of nitroarenes to produce azo compound under mild reaction conditions at 80 °C and 3 MPa H_2 pressure. More important, the catalyst was used for 5 consecutive cycles, and no change in the selectivity or yield was observed.

Cui et al. developed a Pt SA heterogeneous catalyst for hydrosilylation reactions of industrial relevant olefins with the TON of 10^5.[330] To study the Pt-SA catalyst, hydrosilylation reaction of 1-octene and diethoxymethylsilane under solvent-free conditions was used as a model reaction. Model reaction occurred with high anti-Markonikov selectivity and low alkene isomerization compared to previously published data using a homogeneous Pt catalyst. Other control reactions using Pt nanoparticles on an Al_2O_3 nanorod and a commercial Pt/Al_2O_3 catalyst showed low activity. The hydrosilylation reaction allowed control over the hydrophobicity of various surfaces, but the selective formation of the Si−C bond in the presence of different functional groups is challenging and highly desirable for various applications including elastic skin. A Pt-SA catalyst was used for the hydrosilylation of 4-vinyl-1-cyclohexene (2 V) (**Figure 9**a). The Pt-SA exhibited good activity for the unsaturated ester with a yield of 89% and the reaction of 4-allylbenzonitrile with 1a results in the corresponding nitrile with 57% yield (Figure 9a). Notably, Pt-SA catalyst was also employed for hydrosilylation of different alkene (Figure 9b).

The stability and recyclability of selected catalysts showed the recyclability for 6 cycles without any postsynthesis treatment (Figure 9c). To further check the oxygen reactivity of
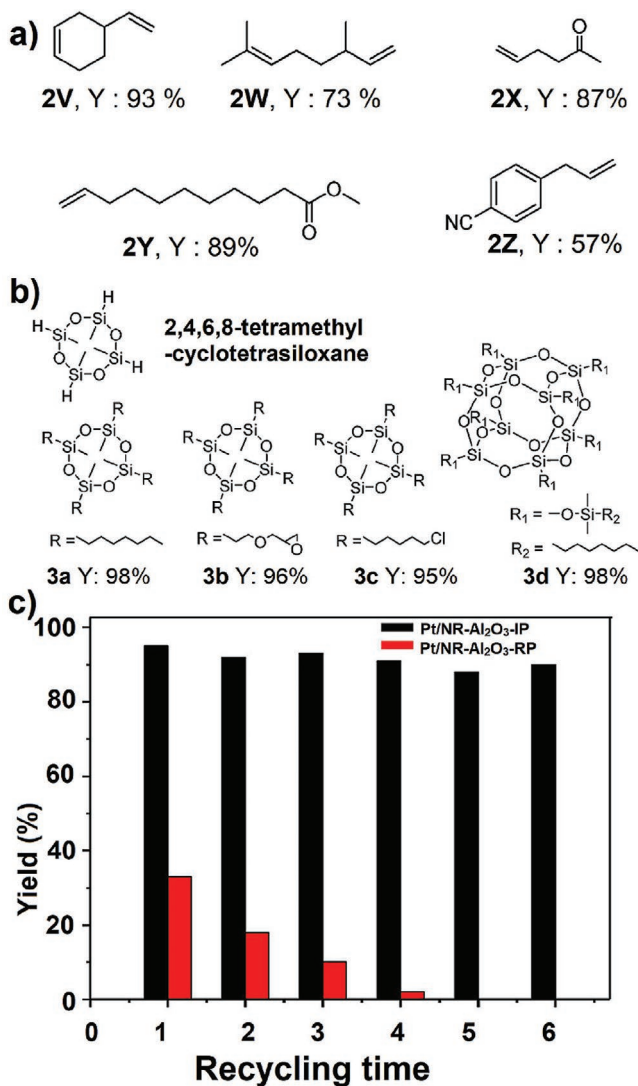

Figure 9. a) Scheme for selective hydrosilylation of alkenes, b) selective hydrosilylation of cyclopentasiloxane and POSS derivatives, c) recyclability of Pt-SA catalyst. Reproduced with permission.[330] Copyright 2017, American Chemical Society.

the Pt-SA sites, a more sensitive oxygen-containing allylic compound such as cyclohexyl vinyl ether, 1,2-epoxy-4-vinyl cyclohexane, and allyl glycidyl ether were also hydroxylated. The catalyst showed tolerance to these sensitive oxygen-containing organic with the desirable yield (around 90%). More interestingly the catalyst even tolerated the epoxy ring in allyl glycidyl ethers which are more susceptible to the ring-opening side reactions. Pt-SA catalyst was also used for the industrially relevant reactions of polysilanes with the olefins. The final products had distinctive optical and electrical properties and may also serve as an important starting precursors for designing novel materials including nanostructured silicon carbide.

The C−H bond selective oxidation is one of the most important organic transformations for making high value-added chemicals such as aldehyde, ketone, ester, and carboxylic acid. However, higher stability of the C−H bond increased the

16

dissociation energy and overoxidation of C—H bonds result in the formation of many side products, selective and low conversion is the main challenges for this organic transformation. Liu et al. developed Fe-SACs supported on N-doped carbon catalyst (Fe-N-C-700) for the selective oxidation of the C—H bond, which exhibited high conversion(98%) and selectivity (97%), and 1932 h^{-1} TOF.[331] The catalyst was also explored for a variety of organic molecules including bulky and sterically hindered substrates such as cumene, diphenylmethane, and fluorene were also activated by using the Fe-N-C-700 catalyst. To stimulate and understanding the landscape of the active sites at the atomic level, KSCN poisoning was conducted because SCN$^-$ can easily make a strong chelated complex with Fe unsaturated sites. Experimental results suggested that the catalyst may have three types of active sites that were observed in Mössbauer spectroscopy. Out of the three different active sites, the N–(Fe^{III}–N$_4$) medium spin was the most active catalytic sites and one order higher active than high spin sixfold D2 (N–Fe^{III}–N$_4$–Y high spin species) and three times more active than the D1 species (Fe^{II}–N$_4$ medium spin species). In Fe-N-C-700, the order of the catalytic activity was D4 >> D2 >> D3. The catalyst was found stable for at least five cycles without showing any changes in the catalytic activity and selectivity.

The C—F bond activation is another interesting chemical transformation from the chemical synthesis and environmental remediation points of view; however, the stability of the C—F bond is the main challenge. To achieve this transformation by a cost-effective and energy-efficient process, a Pt-SA catalyst on SiC was developed.[332] For this study, a persistent environmental pollutant perfluorooctanoic acid was used and the 1.6 wt% Pt loaded SACs showed a photocatalytic rate constant of 2 h^{-1}, which was consistent for a wide range of pH (5.1–9.1). Photocatalytic activity of Pt/SiC catalyst was attributed to i) facile transfer of photoexcited electron in SiC conduction band to Pt$_1$ active sites by Schottky barrier, ii) selective proton reduction and formation of Pt—H bond via Volmer reaction, and iii) efficient hydrogen spillover onto Si-terminals.

In another example of selective organic transformations, Rh$_1$/MoS$_2$ SA catalyst was developed for hydrogenation of crotonaldehyde to crotyl alcohol with 100% selectivity.[333] The catalyst studies suggested that the Rh$_1$/MoS$_2$ might have unique geometry and electronic configuration which confined the reactant molecules through the steric effect. The DFT calculations suggested that the MoS$_2$ sheets oxidized Mo edges and the Rh$_1$-SA was stabilized by a Mo cation vacancy which helped in the H$_2$ adsorption, dissociation into H atoms, and transfers to the double bond for selective hydrogenation. Recently, Zhang et al. used Cu-SA for hydrogenation of quinoline to tetrahydroquinoline with good selectivity (99%) under mild reaction conditions.[334] The catalytic activity of Cu-SA can be controlled by the type of nitrogen (pyrrolic or pyridinic) and pyrrolic N-coordination benefits the hydrogen transfer and reduce the energy barrier of the hydrogenation pathway. In another work, selective chemoselective and regioselective hydrogenation using Pt1/N–C was explored.[335] Twenty-four different metal-SACs were prepared using metalloporphyrin with target metal SA. Recently, Ma et al. also explored Pd-SACs for chemoselective hydrogenation of substituted nitroaromatics (>99%) and gas-phase hydrogenation of CO$_2$ to CO (>98%).[336] Note to worthy,

catalyst showed the excellent thermal stability up to 400 °C without any observable aggregation of SA.

Borrome et al. developed graphene supported Ni-SA catalyst for the C–H activation in the gas phase.[337] Different types of linear branched, and cyclic alkanes were used for the C–H activation and the catalyst was capable of second and third dehydrogenation which led to forming dienes and aromatics such as benzene. Recently, Wan et al. also developed a perovskite-supported Pt-SA catalyst for CH$_4$ activation.[338] Sun et al. explored Pt/Cu SAA for dehydrogenation of propane.[339] Pt-SA dispersed on Cu nanoparticles enhanced desorption of surface-bound propylene selectivity (90%) and excellent thermal stability for 120 h at 520 °C. Recently, PtGa-Pb/SiO$_2$ catalyst was also investigated for dehydrogenation of propane with the 30% conversion with 99.6% selectivity at 600 °C for 96 h,[340] which is higher than the Pt/Cu-SAA catalyst.[339]

Epoxides such as styrene oxide, glycidol, etc. are important intermediates and widely used for many industrial fine chemical preparations, the use of TM-based SA catalyst for industrial relevant processes will further help to achieve the sustainability goals. The gram-scale synthesis of the TM-SA (Fe, Ni, Cu, and Zn) catalyst with high metal loading using pyrolysis of coordinated polymer was exploited for the epoxidation of styrene.[119] O$_2$ has used an only oxidant for epoxidation and Fe-SA catalyst with 30 wt% metal loading showed 64% yield with 89% selectivity, while other control experiments using Fe nanoparticles and iron porphyrin were inactive under the same conditions.

Benzene is one of the most volatile organic molecules that can cause cancer in humans and are organic products produced from petroleum industries; availability can be used to produce another variant of benzene such as phenol. In this regard, Pan et al. developed a FeN$_x$–C$_y$ SA catalyst for the oxidation of benzene to phenol.[341] Fe SA anchored by four N atoms exhibit benzene conversion with 78% and 100% selectivity for phenol. DFT calculation predicted the formation mechanism and the formation of key intermediates. Fe–N$_4$ sites facilitate the activation of O=Fe=O intermediates and increase the catalytic performance of benzene oxidation.

P-coordinated organometallic phosphine complexes have been widely used for many catalytic transformations such as coupling reactions, hydrogenation, carbonylation, etc. Recently, P-coordinated SACs was developed for selective hydrogenation and reductive aminations to the value-added chemicals (**Figure 10**).[342] In this work, a fabrication of surface graphitic phosphorus species (P$_{grap}$)-coordinated Fe SACs (Fe-P900-PCC) through a templated sacrificial approach using phytic acid and Fe precursors (Figure 10a) was performed. The integrated spectroscopy characterization and theoretical calculations confirmed the existence of four P atom coordinated Fe-SA in the pyramidal structure of O$_2$-Fe-P$_4$. Oxygen was removed by hydrogen treatment under optimum conditions which result in Fe-P$_4$ sites. Fe-P900-PCC shows an excellent %conversion for selective amination of aldehyde or ketone (Figure 10b), hydrogenation of substituted nitroarenes (Figure 10c). Fe-P900-PCC had also utilized for the gram-scale drug molecules Buclizine in gram scale and also exhibited excellent stability for varieties of reaction (Figure 10d–f). Pd-SACs was also explored for the Suzuki coupling reaction.[343]
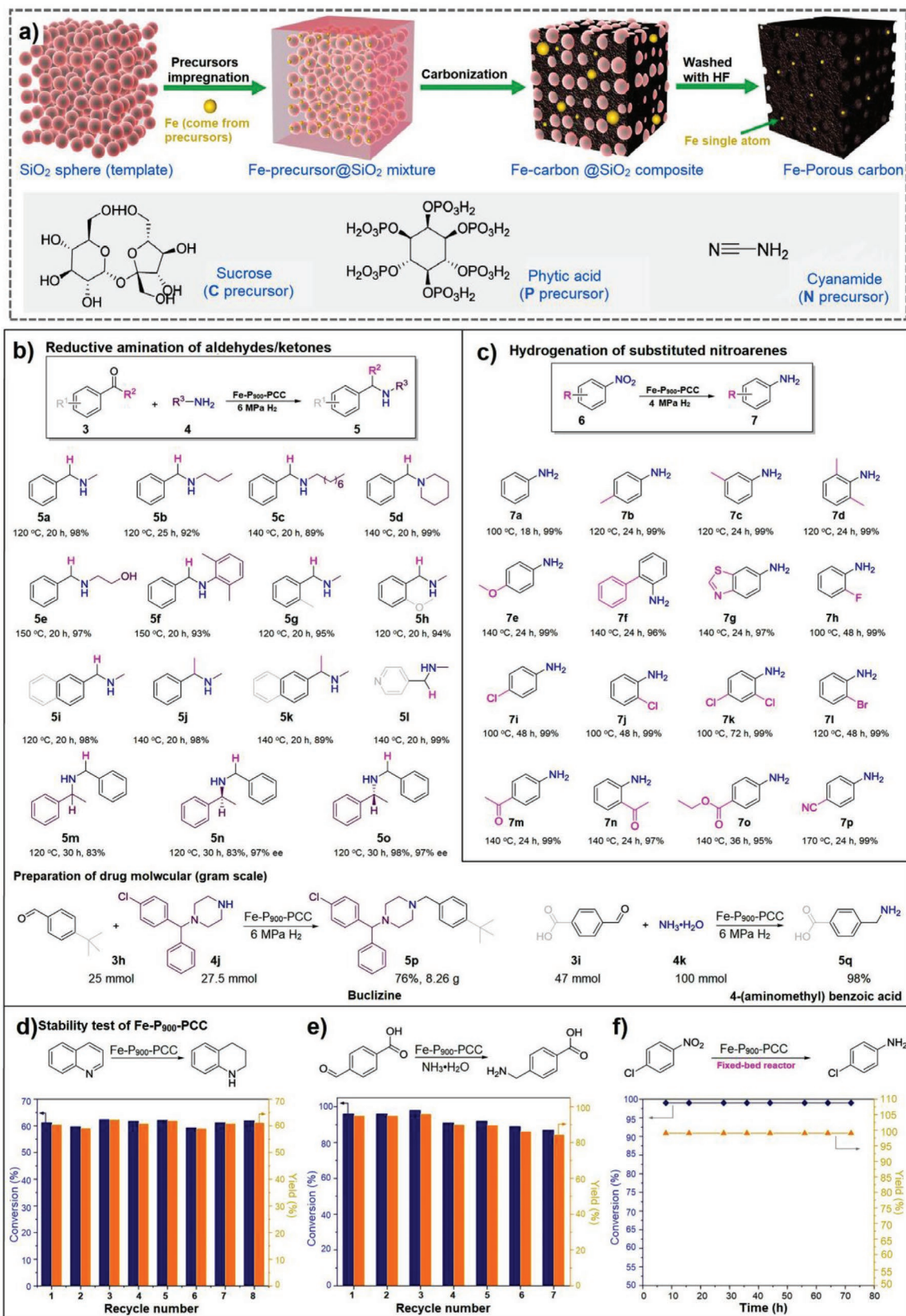
Figure 10. a) Scheme for preparation of PCCs. b,c) Various reactions catalyzed using Fe-P900-PCC. d–f) Stability test of Fe-P900-PCC. Reproduced with permission.[342] Copyright 2020, Nature Publishing Group.

The theoretical perspectives are very important for obtaining a fundamental mechanistic understanding of the catalytic process. Theoretical modeling of the catalytic process and optimization of SA using different TM and operational conditions for a particular reaction can help to decrease the overall process time and also save resources. Hence now a days, theoretical calculations before the experimental process can help to design a specific SA catalyst and will further enhance the time utility.[344,345] Therefore, for theoretical modeling, consideration of real operational conditions is necessary, even though some of the operating conditions may not be possible to include in modeling, due to their complex nature.[197] Kong et al. theoretically confirmed that vanadium atoms were anchored on graphitic carbon nitride for nonoxidative propane dehydrogenation.[346] The high activity of V_1/g-C_3N_4 was attributed to low coordination 3d orbital of V atoms, while propylene selectivity was initiated from inhibition of di-σ binding mode of propylene on single V atoms.

4. Conclusion

We summarized key examples of SACs for ORR, OER, HER, metal–air batteries, and electrochemical organic transformations. The development of electrocatalysts using noble and non-noble metals and their applications over the last few years were discussed. For the development of SACs, significant progress has been made in terms of large-scale synthesis, understanding the electrocatalytic phenomena and mechanism at the fundamental level, the role of the metal support, and bimetallic system on the activity and selectivity. The selectivity and catalytic properties that are mainly driven by the electronic environment of the SA can be tuned via a combination of support, heteroatoms doping and using the multimetallic system. Theoretical work is also conducted to understanding of electrocatalytic mechanism at the molecular level, major progress has been made in this regard. The development of an efficient protocol to produce low metal loading catalysts at the atomic level on a large scale is highly desirable. The catalyst prepared from the industrial metal waste sources should be an obvious choice to make a circular economy. Integration of an electrochemical device with electricity from renewable sources is another key step to making a greener future; however, while calculating the carbon footprint, it is necessary to include the cost of renewable energy generation.

5. Future Directions and Applications

Concerns about the environment have been continuously increasing, which is due to an increase in energy demand and globalization. To meet the energy demand and achieve environmental remediation, we need to develop an efficient and sustainable protocol to generate a large amount of energy without further degrading and contaminating the environment. SACs are the most efficient catalyst produced so far. Nevertheless, we are still facing some challenges about SACs long-term reusability and stability. In this section, we take an opportunity to highlight the possible future applications of SACs which have not been explored yet or either not discussed in detail. For further focus, we need to concentrate on some important fields which need to be addressed urgently.

1. Rational design of SACs: Engineering the rational design for large-scale production of SACs is highly desirable for its key advancement in various fields.[347] Several theoretical[128,348–350] and experimental models[351–353] are given for SACs rational designs. Besides these predictable models, understanding the catalytic activity and its composition relation is highly complex and challenging. It is simply unbearable to test all the relevant catalyst combinations for the desired reaction when catalyst involved a combination of several types of active sites (different active sites structures) and compositions (support and bimetallic to multimetallic), and size (SA to cluster of several single atoms).[145,354,355] These factors are strongly dependents on one another and catalytic activity could be the combination of all influencers. However, a systematic approach could lead to overcome all the barriers and allow to design of rational catalysts.

2. Densely packed SACs: The synthesis of SACs with high metal loading is highly demanding for various industrial applications. However, the fabrication of such material is highly challenging, due to the limitation of various synthesis procedures. For example, conventional pyrolysis protocol usually leads to the agglomeration of SA to bigger nanoparticles. Although, several other methods are reported, still have limited to metal loading lesser than 10 wt%.[356–358] Very few reports are published with the metal loading greater than 10 wt%.[73,180,359,360] Despite the satisfactory progress in the synthesis of dense SACs, it remains difficult to control the type and distribution of active sites.

3. Thermal stability of SACs: Thermal stability of SACs is a big issue and utilization of SACs at elevated temperature is highly desired.[192,361] To keep them isolated, the operational temperature is typically kept below 300 °C.[362] Few examples were reported to explore SACs for industrial relevant high temperature (>300 °C) gas-phase applications.[336,339,340,363] The thermal stability of SACs can be enhanced by strong interaction through a strong covalent metal–support interaction.[46] The controllable high-temperature shockwave strategy,[364] atom trapping,[365] and entropy-driven[366] methods were utilized to stabilize SA. Periodic on–off heating for short time (55 ms) allowed the formation of thermodynamically favorable strong metal-defect bonds.[364] Recently, temperature-induced structure reconstruction of support was explored to synthesize high-temperature stable SACs at 800 °C.[367]

4. Fundamental understanding of SACs (atomic level information): SACs have been widely employed for many reactions and now seem clear that supported metal atoms can effectively catalyzed challenging reactions. Most of the reported to date particularly talk about the synthesis, stability, and increasing the metal loading, but how the coordination environment or structures of active site geometry affect overall performance is still an open question.[368] The coordination environments around the SA can be tuned by various heteroatom doping and by the use of different neighbor metal atoms which brings thousands of possibilities of different combinations. During the catalyst preparation, homogenization of active

sites is highly challenging, and as prepared catalyst always have varieties of active sites. It could be possible that different molecular sites have different activity and selectivity for the same reactions which are hard to estimate at the atomic level. Also, support metal interaction has a great impact on the catalytic properties, sometimes support atoms or surface functional groups help in stabilizing some of the intermediates, which help in facilitating the catalytic cycles. Surface sensitive techniques such as XPS could be useful and support of DFT modeling is also equally important.[369]

5. Use of electric vehicles for transport and personal uses: Due to the continuous decline of petroleum resources, it is necessary to quest for alternative electric vehicles; batteries are only a time-limited source of energy for now. Although extensive work has been done on improving different aspects of batteries low-cost; and recyclable; environmentally benign materials are a necessity.[261] Efficient and cost-effective SACs for metal–air batteries are needed to meet the battery's demand.

6. CO_2 capture and conversion at hot spot: Continuously increase of CO_2 levels in the environment is possessing danger for living beings. Direct air capture and postcombustion capture and conversion are highly demanded and millions of funds have been recently made available to develop an efficient and workable technology to deal with CO_2. Although many industries focus on capture and storage, this is not a viable long-term solution. We should capture CO_2 and parallel convert into value-added products such as fuel or polymer.[370] Recently many reports have been published highlighting SACs for CO_2 conversion,[371] but none of them met the industrial requirement, which needs to be focused on more.[372]

7. Capture CO_2 using a solid electrochemical system: An electrochemical cell is a device of solid capture media with the electrode assembly, which captures CO_2 when charged and released on discharge. Recently, an electrochemical setup for direct CO_2 capture has been demonstrated. It was able to capture low as 0.6% (6000 ppm) concentration of CO_2.[373,374] Al Sadat and Archer demonstrated an O_2-assisted Al/CO_2 electrochemical cell as a new strategy for CO_2 capture, which can at the same time be generated a substantial amount of electric energy.[375] The cathode provides a valuable C_2 species and electric energy. The first cell reduced O_2 to superoxide intermediate and simultaneously reacted with CO_2 in the form of aluminum oxalate $Al_2(C_2O_4)_3$, as a dominant product. This process may be possible to accelerate using SACs doped Al-cathode.

8. Electrocatalyst for NO_X and SO_x: A catalytic converter is a catalytic device attached to exhaust and convert harmful gases such as NO_X, CO, and VOC in N_2, O_2, and CO_2. In this series, a selective catalytic converter (SCR) is an advanced emission control device that injects a liquid-reductant agent into the exhaust stream to reduce the level of NO_X in the exhaust. SCR selective use ammonia to convert NO_X to N_2 and O_2. Mostly these catalysts are made of Rh, Pt, and Pd; the catalytic activity may further be accelerated by developing an SACs solid electrolyte cell.[376] Recently, direct reduction of NO with CO into N_2 and CO_2 using Ni-SACs investigated using a theoretical model.[377]

9. Dechlorination of environmental contamination: Organics like chloromethane, methylene chloride, chloroform, and carbon tetrachloride are the major solvents used by paint and Pharmaceutical industries worldwide. The excessive release of the solvent into the environment not only harms our health but also dramatically affects the ozone layer by a catalytic chain reaction. A heterogeneous catalyst is used for dechlorination of water and air, which can be further improved by developing SACs. This process can be further accelerated by using electrochemical cells.[378]

Conflict of Interest

The authors declare no conflict of interest.

[1] D. S. Doke, J. H. Advani, D. R. Naikwadi, M. B. Gawande, P. Walke, S. B. Umbarkar, A. V. Biradar, *ACS Sustain. Chem. Eng* **2019**, *7*, 3018.

[2] M. B. Gawande, A. Goswami, F.-X. Felpin, T. Asefa, X. Huang, R. Silva, X. Zou, R. Zbořil, R. S. Varma, *Chem. Rev.* **2016**, *116*, 3722.

[3] A. S. Burange, M. B. Gawande, F. L. Y. Lam, R. V. Jayaram, R. Luque, *Green Chem.* **2015**, *17*, 146.

[4] C. S. K. Lin, L. A. Pfaltzgraff, L. Herrero-Davila, E. B. Mubofu, S. Abderrahim, J. H. Clark, A. A. Koutinas, N. Kopsahelis, K. Stamatelatou, F. Dickson, S. Thankappan, Z. Mohamed, R. Brocklesby, R. Luque, *Energy Environ. Sci.* **2013**, *6*, 426.

[5] M. Melchionna, P. Fornasiero, *ChemCatChem* **2017**, *9*, 3274.

[6] M. B. Gawande, P. S. Branco, R. S. Varma, *Chem. Soc. Rev.* **2013**, *42*, 3371.

[7] F. Dumeignil, J.-F. Paul, S. Paul, *J. Chem. Edu.* **2017**, *94*, 675.

[8] X. Chia, M. Pumera, *Nat. Catal.* **2018**, *1*, 909.

[9] A. Kumar, Q. Xu, *ChemNanoMat* **2018**, *4*, 28.

[10] C. Lin, H. Zhang, X. Song, D.-H. Kim, X. Li, Z. Jiang, J.-H. Lee, *Mater. Horiz.* **2020**, *7*, 2726.

[11] W. Xiong, H. Li, H. Wang, J. Yi, H. You, S. Zhang, Y. Hou, M. Cao, T. Zhang, R. Cao, *Small* **2020**, *16*, 2003943.

[12] Y. Han, Y.-G. Wang, W. Chen, R. Xu, L. Zheng, J. Zhang, J. Luo, R.-A. Shen, Y. Zhu, W.-C. Cheong, C. Chen, Q. Peng, D. Wang, Y. Li, *J. Am. Chem. Soc.* **2017**, *139*, 17269.

[13] E. Gross, J. H.-C. Liu, F. D. Toste, G. A. Somorjai, *Nat. Chem.* **2012**, *4*, 947.

[14] P. Christopher, S. Linic, *J. Am. Chem. Soc.* **2008**, *130*, 11264.

[15] S. K. Kaiser, Z. Chen, D. Faust Akl, S. Mitchell, J. Pérez-Ramírez, *Chem. Rev.* **2020**, *120*, 11703.

[16] Q. Fu, H. Saltsburg, M. Flytzani-Stephanopoulos, *Science* **2003**, *301*, 935.

[17] R. Bashyam, P. Zelenay, *Nature* **2006**, *443*, 63.

[18] I. Thomé, A. Nijs, C. Bolm, *Chem. Soc. Rev.* **2012**, *41*, 979.

[19] C. K. Chua, M. Pumera, *Chem. - Eur. J.* **2015**, *21*, 12550.

[20] B. Qiao, A. Wang, X. Yang, L. F. Allard, Z. Jiang, Y. Cui, J. Liu, J. Li, T. Zhang, *Nat. Chem.* **2011**, *3*, 634.

[21] G. Centi, S. Perathoner, *Catal. Today* **2003**, *77*, 287.

[22] W. Wu, L. Huang, E. Wang, S. Dong, *Chem. Sci.* **2020**, *11*, 9741.

[23] R. J. P. Williams, *Chem. Commun.* **2003**, 1109.

[24] B. Cornils, W. A. Herrmann, *J. Catal.* **2003**, *216*, 23.

[25] L. Jiao, H. Yan, Y. Wu, W. Gu, C. Zhu, D. Du, Y. Lin, *Angew. Chem. Int. Ed.* **2020**, *59*, 2565.

[26] A. Wang, J. Li, T. Zhang, *Nat. Rev. Chem.* **2018**, *2*, 65.

[27] C. Zhu, S. Fu, Q. Shi, D. Du, Y. Lin, *Angew. Chem. Int. Ed.* **2017**, *56*, 13944.

[28] H. Zhang, G. Liu, L. Shi, J. Ye, *Adv. Energy Mater.* **2018**, *8*, 1701343.

[29] C. Rivera-Cárcamo, P. Serp, *ChemCatChem* **2018**, *10*, 5058.

[30] J. Su, R. Ge, Y. Dong, F. Hao, L. Chen, *J. Mater. Chem. A* **2018**, *6*, 14025.

[31] S. Weon, D. Huang, K. Rigby, C. Chu, X. Wu, J.-H. Kim, *ACS ES&T Eng.* **2020**, https://doi.org/10.1021/acsestengg.0c00136.

[32] C. H. Choi, M. Kim, H. C. Kwon, S. J. Cho, S. Yun, H.-T. Kim, K. J. J. Mayrhofer, H. Kim, M. Choi, *Nat. Commun.* **2016**, *7*, 10922.

[33] J. Lin, A. Wang, B. Qiao, X. Liu, X. Yang, X. Wang, J. Liang, J. Li, J. Liu, T. Zhang, *J. Am. Chem. Soc.* **2013**, *135*, 15314.

[34] H. Yan, H. Cheng, H. Yi, Y. Lin, T. Yao, C. Wang, J. Li, S. Wei, J. Lu, *J. Am. Chem. Soc.* **2015**, *137*, 10484.

[35] Y. Chen, S. Ji, Y. Wang, J. Dong, W. Chen, Z. Li, R. Shen, L. Zheng, Z. Zhuang, D. Wang, Y. Li, *Angew. Chem. Int. Ed.* **2017**, *56*, 6937.

[36] H. Li, L. Wang, Y. Dai, Z. Pu, Z. Lao, Y. Chen, M. Wang, X. Zheng, J. Zhu, W. Zhang, R. Si, C. Ma, J. Zeng, *Nat. Nanotechnol.* **2018**, *13*, 411.

[37] M. Piernavieja-Hermida, Z. Lu, A. White, K.-B. Low, T. Wu, J. W. Elam, Z. Wu, Y. Lei, *Nanoscale* **2016**, *8*, 15348.

[38] S. Abbet, A. Sanchez, U. Heiz, W. D. Schneider, A. M. Ferrari, G. Pacchioni, N. Rösch, *J. Am. Chem. Soc.* **2000**, *122*, 3453.

[39] Y. Qu, B. Chen, Z. Li, X. Duan, L. Wang, Y. Lin, T. Yuan, F. Zhou, Y. Hu, Z. Yang, C. Zhao, J. Wang, C. Zhao, Y. Hu, G. Wu, Q. Zhang, Q. Xu, B. Liu, P. Gao, R. You, W. Huang, L. Zheng, L. Gu, Y. Wu, Y. Li, *J. Am. Chem. Soc.* **2019**, *141*, 4505.

[40] H. Yang, L. Shang, Q. Zhang, R. Shi, G. I. N. Waterhouse, L. Gu, T. Zhang, *Nat. Commun.* **2019**, *10*, 4585.

[41] X. Ao, W. Zhang, Z. Li, J.-G. Li, L. Soule, X. Huang, W.-H. Chiang, H. M. Chen, C. Wang, M. Liu, X. C. Zeng, *ACS Nano* **2019**, *13*, 11853.

[42] L. Yang, D. Cheng, H. Xu, X. Zeng, X. Wan, J. Shui, Z. Xiang, D. Cao, *Proc. Natl. Acad. Sci. USA* **2018**, *115*, 6626.

[43] C. Zhu, Q. Shi, B. Z. Xu, S. Fu, G. Wan, C. Yang, S. Yao, J. Song, H. Zhou, D. Du, S. P. Beckman, D. Su, Y. Lin, *Adv. Energy Mater.* **2018**, *8*, 1801956.

[44] J.-C. Li, M. Cheng, T. Li, L. Ma, X. Ruan, D. Liu, H.-M. Cheng, C. Liu, D. Du, Z. Wei, Y. Lin, M. Shao, *J. Mater. Chem. A* **2019**, *7*, 14478.

[45] Z. Yang, Y. Wang, M. Zhu, Z. Li, W. Chen, W. Wei, T. Yuan, Y. Qu, Q. Xu, C. Zhao, X. Wang, P. Li, Y. Li, Y. Wu, Y. Li, *ACS Catal.* **2019**, *9*, 2158.

[46] R. Lang, W. Xi, J.-C. Liu, Y.-T. Cui, T. Li, A. F. Lee, F. Chen, Y. Chen, L. Li, L. Li, J. Lin, S. Miao, X. Liu, A.-Q. Wang, X. Wang, J. Luo, B. Qiao, J. Li, T. Zhang, *Nat. Commun.* **2019**, *10*, 234.

[47] Y. Ren, Y. Tang, L. Zhang, X. Liu, L. Li, S. Miao, D. Sheng Su, A. Wang, J. Li, T. Zhang, *Nat. Commun.* **2019**, *10*, 4500.

[48] P. Yin, T. Yao, Y. Wu, L. Zheng, Y. Lin, W. Liu, H. Ju, J. Zhu, X. Hong, Z. Deng, G. Zhou, S. Wei, Y. Li, *Angew. Chem. Int. Ed.* **2016**, *55*, 10800.

[49] F. R. Lucci, J. Liu, M. D. Marcinkowski, M. Yang, L. F. Allard, M. Flytzani-Stephanopoulos, E. C. H. Sykes, *Nat. Commun.* **2015**, *6*, 8550.

[50] V. T. T. Ho, C.-J. Pan, J. Rick, W.-N. Su, B.-J. Hwang, *J. Am. Chem. Soc.* **2011**, *133*, 11716.

[51] J. Timoshenko, B. Roldan Cuenya, *Chem. Rev.* **2020**, https://doi.org/10.1021/acs.chemrev.0c00396.

[52] L. DeRita, S. Dai, K. Lopez-Zepeda, N. Pham, G. W. Graham, X. Pan, P. Christopher, *J. Am. Chem. Soc.* **2017**, *139*, 14150.

[53] X. Li, X. Yang, J. Zhang, Y. Huang, B. Liu, *ACS Catal.* **2019**, *9*, 2521.

[54] J.-X. Liang, J. Lin, X.-F. Yang, A.-Q. Wang, B.-T. Qiao, J. Liu, T. Zhang, J. Li, *J. Phys. Chem. C* **2014**, *118*, 21945.

[55] S. Sun, G. Zhang, N. Gauquelin, N. Chen, J. Zhou, S. Yang, W. Chen, X. Meng, D. Geng, M. N. Banis, R. Li, S. Ye, S. Knights, G. A. Botton, T.-K. Sham, X. Sun, *Sci. Rep.* **2013**, *3*, 1775.

[56] L. Wang, S. Zhang, Y. Zhu, A. Patlolla, J. Shan, H. Yoshida, S. Takeda, A. I. Frenkel, F. Tao, *ACS Catal.* **2013**, *3*, 1011.

[57] X. Li, H.-Y. Wang, H. Yang, W. Cai, S. Liu, B. Liu, *Small Methods* **2018**, *2*, 1700395.

[58] Y. Zhu, J. Wang, H. Chu, Y.-C. Chu, H. M. Chen, *ACS Energy Lett.* **2020**, *5*, 1281.

[59] J. Dou, Z. Sun, A. A. Opalade, N. Wang, W. Fu, F. Tao, *Chem. Soc. Rev.* **2017**, *46*, 2001.

[60] T. Zhao, Y. Wang, S. Karuturi, K. Catchpole, Q. Zhang, C. Zhao, *Carbon Energy* **2020**, *2*, 582.

[61] H.-T. Lien, S.-T. Chang, P.-T. Chen, D. P. Wong, Y.-C. Chang, Y.-R. Lu, C.-L. Dong, C.-H. Wang, K.-H. Chen, L.-C. Chen, *Nat. Commun.* **2020**, *11*, 4233.

[62] M. J. Hülsey, B. Zhang, Z. Ma, H. Asakura, D. A. Do, W. Chen, T. Tanaka, P. Zhang, Z. Wu, N. Yan, *Nat. Commun.* **2019**, *10*, 1330.

[63] A. D. Handoko, F. Wei, B. S. Yeo Jenndy, Z. W. Seh, *Nat. Catal.* **2018**, *1*, 922.

[64] T. Wang, Q. Zhao, Y. Fu, C. Lei, B. Yang, Z. Li, L. Lei, G. Wu, Y. Hou, *Small Methods* **2019**, *3*, 1900210.

[65] C. Wan, X. Duan, Y. Huang, *Adv. Energy Mater.* **2020**, *10*, 1903815.

[66] B. Lu, Q. Liu, S. Chen, *ACS Catal.* **2020**, *10*, 7584.

[67] K. Kamiya, *Chem. Sci.* **2020**, *11*, 8339.

[68] H. Fei, J. Dong, D. Chen, T. Hu, X. Duan, I. Shakir, Y. Huang, X. Duan, *Chem. Soc. Rev.* **2019**, *48*, 5207.

[69] J. Gao, B. Liu, *ACS Mater. Lett.* **2020**, *2*, 1008.

[70] X. Zhu, C. Hu, R. Amal, L. Dai, X. Lu, *Energy Environ. Sci.* **2020**, *13*, 4536.

[71] Y. Wang, F.-L. Hu, Y. Mi, C. Yan, S. Zhao, *Chem. Eng. J.* **2021**, *406*, 127135.

[72] J. Liu, H. Zhang, M. Qiu, Z. Peng, M. K. H. Leung, W.-F. Lin, J. Xuan, *J. Mater. Chem. A* **2020**, *8*, 2222.

[73] J. Wu, L. Xiong, B. Zhao, M. Liu, L. Huang, *Small Methods* **2020**, *4*, 1900540.

[74] M. Li, H. Wang, W. Luo, P. C. Sherrell, J. Chen, J. Yang, *Adv. Mater.* **2020**, *32*, 2001848.

[75] B. Mohanty, B. K. Jena, S. Basu, *ACS Omega* **2020**, *5*, 1287.

[76] C.-C. Hou, H.-F. Wang, C. Li, Q. Xu, *Energy Environ. Sci.* **2020**, *13*, 1658.

[77] Z. Song, L. Zhang, K. Doyle-Davis, X. Fu, J.-L. Luo, X. Sun, *Adv. Energy Mater.* **2020**, *10*, 2001561.

[78] X. Li, L. Liu, X. Ren, J. Gao, Y. Huang, B. Liu, *Sci. Adv.* **2020**, *6*, 6833.

[79] R. Kamai, K. Kamiya, K. Hashimoto, S. Nakanishi, *Angew. Chem. Int. Ed.* **2016**, *55*, 13184.

[80] Y. Xiong, J. Dong, Z.-Q. Huang, P. Xin, W. Chen, Y. Wang, Z. Li, Z. Jin, W. Xing, Z. Zhuang, J. Ye, X. Wei, R. Cao, L. Gu, S. Sun, L. Zhuang, X. Chen, H. Yang, C. Chen, Q. Peng, C.-R. Chang, D. Wang, Y. Li, *Nat. Nanotechnol.* **2020**, *15*, 390.

[81] X. Li, A.-E. Surkus, J. Rabeah, M. Anwar, S. Dastigir, H. Junge, A. Brückner, M. Beller, *Angew. Chem. Int. Ed.* **2020**, *59*, 15849.

[82] O. Y. Podyacheva, D. A. Bulushev, A. N. Suboch, D. A. Svintsitskiy, A. S. Lisitsyn, E. Modin, A. Chuvilin, E. Y. Gerasimov, V. I. Sobolev, V. N. Parmon, *ChemSusChem* **2018**, *11*, 3724.

[83] M. D. Marcinkowski, S. F. Yuk, N. Doudin, R. S. Smith, M.-T. Nguyen, B. D. Kay, V.-A. Glezakou, R. Rousseau, Z. Dohnálek, *ACS Catal.* **2019**, *9*, 10977.

[84] Z. Jiang, X. Feng, J. Deng, C. He, M. Douthwaite, Y. Yu, J. Liu, Z. Hao, Z. Zhao, *Adv. Funct. Mater.* **2019**, *29*, 1902041.

[85] J. C. Calderón, G. García, L. Calvillo, J. L. Rodríguez, M. J. Lázaro, E. Pastor, *Appl. Catal. B* **2015**, *165*, 676.

[86] F. Li, L. Li, X. Liu, X. C. Zeng, Z. Chen, *ChemPhysChem* **2016**, *17*, 3170.

[87] S. Wang, J. Li, Q. Li, X. Bai, J. Wang, *Nanoscale* **2020**, *12*, 364.

[88] Y. Lu, J. Wang, L. Yu, L. Kovarik, X. Zhang, A. S. Hoffman, A. Gallo, S. R. Bare, D. Sokaras, T. Kroll, V. Dagle, H. Xin, A. M. Karim, *Nat. Catal.* **2019**, *2*, 149.

[89] S. Back, J. Lim, N.-Y. Kim, Y.-H. Kim, Y. Jung, *Chem. Sci.* **2017**, *8*, 1090.

[90] X.-L. Lu, X. Rong, C. Zhang, T.-B. Lu, *J. Mater. Chem. A* **2020**, *8*, 10695.

[91] H. Zou, W. Rong, S. Wei, Y. Ji, L. Duan, *Proc. Natl. Acad. Sci. USA* **2020**, *117*, 29462.

[92] X. Liu, Y. Jiao, Y. Zheng, M. Jaroniec, S.-Z. Qiao, *J. Am. Chem. Soc.* **2019**, *141*, 9664.

[93] N. Cao, Z. Chen, K. Zang, J. Xu, J. Zhong, J. Luo, X. Xu, G. Zheng, *Nat. Commun.* **2019**, *10*, 2877.

[94] M. Li, H. Huang, J. Low, C. Gao, R. Long, Y. Xiong, *Small Methods* **2019**, *3*, 1800388.

[95] R. Xiao, K. Chen, X. Zhang, Z. Yang, G. Hu, Z. Sun, H.-M. Cheng, F. Li, *J. Energy Chem.* **2021**, *54*, 452.

[96] F. Wang, J. Li, J. Zhao, Y. Yang, C. Su, Y. L. Zhong, Q.-H. Yang, J. Lu, *ACS Mater. Lett.* **2020**, *2*, 1450.

[97] C. Lu, R. Fang, X. Chen, *Adv. Mater.* **2020**, *32*, 1906548.

[98] K. Kaneda, T. Mizugaki, *ACS Catal.* **2017**, *7*, 920.

[99] M. B. Gawande, V. D. B. Bonifácio, R. Luque, P. S. Branco, R. S. Varma, *Chem. Soc. Rev.* **2013**, *42*, 5522.

[100] L. Ilies, S. P. Thomas, I. A. Tonks, *Asian J. Org. Chem.* **2020**, *9*, 324.

[101] D. Wang, D. Astruc, *Chem. Soc. Rev.* **2017**, *46*, 816.

[102] F. Zaera, *ChemSusChem* **2013**, *6*, 1797.

[103] S. Saddeler, U. Hagemann, S. Schulz, *Inorg. Chem.* **2020**, *59*, 10013.

[104] M. Mandić, B. Todić, L. Živanić, N. Nikačević, D. B. Bukur, *Ind. Eng. Chem. Res.* **2017**, *56*, 2733.

[105] M. Shao, A. Peles, K. Shoemaker, *Nano Lett.* **2011**, *11*, 3714.

[106] S. Cao, F. Tao, Y. Tang, Y. Li, J. Yu, *Chem. Soc. Rev.* **2016**, *45*, 4747.

[107] L. Liu, A. Corma, *Chem. Rev.* **2018**, *118*, 4981.

[108] C. Xie, Z. Niu, D. Kim, M. Li, P. Yang, *Chem. Rev.* **2020**, *120*, 1184.

[109] M. K. Samantaray, V. D'Elia, E. Pump, L. Falivene, M. Harb, S. Ould Chikh, L. Cavallo, J.-M. Basset, *Chem. Rev.* **2020**, *120*, 734.

[110] A. Bakandritsos, R. G. Kadam, P. Kumar, G. Zoppellaro, M. Medved, J. Tuček, T. Montini, O. Tomanec, P. Andrýsková, B. Drahoš, R. S. Varma, M. Otyepka, M. B. Gawande, P. Fornasiero, R. Zbořil, *Adv. Mater.* **2019**, *31*, 1900323.

[111] Y. Lei, H. Zhao, R. D. Rivas, S. Lee, B. Liu, J. Lu, E. Stach, R. E. Winans, K. W. Chapman, J. P. Greeley, J. T. Miller, P. J. Chupas, J. W. Elam, *J. Am. Chem. Soc.* **2014**, *136*, 9320.

[112] P. F. Siril, L. Ramos, P. Beaunier, P. Archirel, A. Etcheberry, H. Remita, *Chem. Mater.* **2009**, *21*, 5170.

[113] B. B. Sarma, P. N. Plessow, G. Agostini, P. Concepción, N. Pfänder, L. Kang, F. R. Wang, F. Studt, G. Prieto, *J. Am. Chem. Soc.* **2020**, *142*, 14890.

[114] T. Bligaard, J. K. Nørskov, *Electrochim. Acta* **2007**, *52*, 5512.

[115] L. Liu, A. Corma, *Trends Chem.* **2020**, *2*, 383.

[116] L. Liu, D. M. Meira, R. Arenal, P. Concepcion, A. V. Puga, A. Corma, *ACS Catal.* **2019**, *9*, 10626.

[117] E. M. Fernández, J. M. Soler, I. L. Garzón, L. C. Balbás, *Phys. Rev. B* **2004**, *70*, 165403.

[118] S. Schauermann, J. Hoffmann, V. Johánek, J. Hartmann, J. Libuda, H.-J. Freund, *Angew. Chem. Int. Ed.* **2002**, *41*, 2532.

[119] Y. Xiong, W. Sun, P. Xin, W. Chen, X. Zheng, W. Yan, L. Zheng, J. Dong, J. Zhang, D. Wang, Y. Li, *Adv. Mater.* **2020**, *32*, 2000896.

[120] J.-C. Liu, X. Hiao, J. Li, *J. Am. Chem. Soc.* **2020**, *142*, 3375.

[121] Y. Du, H. Sheng, D. Astruc, M. Zhu, *Chem. Rev.* **2020**, *120*, 526.

[122] T. Ren, M. K. Patel, *Resour. Conserv. Recycl.* **2009**, *53*, 513.

[123] I. Staffell, D. Scamman, A. Velazquez Abad, P. Balcombe, P. E. Dodds, P. Ekins, N. Shah, K. R. Ward, *Energy Environ. Sci.* **2019**, *12*, 463.

[124] I. Dincer, M. A. Rosen, *Energy Sustain. Dev.* **2011**, *15*, 137.

[125] Y. Jiao, Y. Zheng, M. Jaroniec, S. Z. Qiao, *Chem. Soc. Rev.* **2015**, *44*, 2060.

[126] J. Kim, H.-E. Kim, H. Lee, *ChemSusChem* **2018**, *11*, 104.

[127] L. Zhang, K. Doyle-Davis, X. Sun, *Energy Environ. Sci.* **2019**, *12*, 492.

[128] H. Xu, D. Cheng, D. Cao, X. C. Zeng, *Nat. Catal.* **2018**, *1*, 339.

[129] J. Liu, M. Jiao, B. Mei, Y. Tong, Y. Li, M. Ruan, P. Song, G. Sun, L. Jiang, Y. Wang, Z. Jiang, L. Gu, Z. Zhou, W. Xu, *Angew. Chem. Int. Ed.* **2019**, *58*, 1163.

[130] Z. Guo, Y. Xie, J. Xiao, Z.-J. Zhao, Y. Wang, Z. Xu, Y. Zhang, L. Yin, H. Cao, J. Gong, *J. Am. Chem. Soc.* **2019**, *141*, 12005.

[131] D. Zhao, Z. Zhuang, X. Cao, C. Zhang, Q. Peng, C. Chen, Y. Li, *Chem. Soc. Rev.* **2020**, *49*, 2215.

[132] J. Liu, M. Jiao, L. Lu, H. M. Barkholtz, Y. Li, Y. Wang, L. Jiang, Z. Wu, D.-j. Liu, L. Zhuang, C. Ma, J. Zeng, B. Zhang, D. Su, P. Song, W. Xing, W. Xu, Y. Wang, Z. Jiang, G. Sun, *Nat. Commun.* **2017**, *8*, 15938.

[133] X. Zeng, J. Shui, X. Liu, Q. Liu, Y. Li, J. Shang, L. Zheng, R. Yu, *Adv. Energy Mater.* **2018**, *8*, 1701345.

[134] M. Melchionna, P. Fornasiero, M. Prato, *Adv. Mater.* **2019**, *31*, 1802920.

[135] S. Yang, J. Kim, Y. J. Tak, A. Soon, H. Lee, *Angew. Chem. Int. Ed.* **2016**, *55*, 2058.

[136] S. Yang, Y. J. Tak, J. Kim, A. Soon, H. Lee, *ACS Catal.* **2017**, *7*, 1301.

[137] R. Shen, W. Chen, Q. Peng, S. Lu, L. Zheng, X. Cao, Y. Wang, W. Zhu, J. Zhang, Z. Zhuang, C. Chen, D. Wang, Y. Li, *Chem* **2019**, *5*, 2099.

[138] C. Deng, R. He, W. Shen, M. Li, *Phys. Chem. Chem. Phys.* **2019**, *21*, 18589.

[139] H.-W. Liang, W. Wei, Z.-S. Wu, X. Feng, K. Müllen, *J. Am. Chem. Soc.* **2013**, *135*, 16002.

[140] S. Fang, X. Zhu, X. Liu, J. Gu, W. Liu, D. Wang, W. Zhang, Y. Lin, J. Lu, S. Wei, Y. Li, T. Yao, *Nat. Commun.* **2020**, *11*, 1029.

[141] L. Huang, J. Chen, L. Gan, J. Wang, S. Dong, *Sci. Adv.* **2019**, *5*, eaav5490.

[142] W. Chen, W. Gao, P. Tu, T. Robert, Y. Ma, H. Shan, X. Gu, W. Shang, P. Tao, C. Song, T. Deng, H. Zhu, X. Pan, H. Yang, J. Wu, *Nano Lett.* **2018**, *18*, 5905.

[143] L. Zhang, H. Liu, S. Liu, M. Norouzi Banis, Z. Song, J. Li, L. Yang, M. Markiewicz, Y. Zhao, R. Li, M. Zheng, S. Ye, Z.-J. Zhao, G. A. Botton, X. Sun, *ACS Catal.* **2019**, *9*, 9350.

[144] R. T. Hannagan, G. Giannakakis, M. Flytzani-Stephanopoulos, E. C. H. Sykes, *Chem. Rev.* **2020**, *120*, 12044.

[145] G. Giannakakis, M. Flytzani-Stephanopoulos, E. C. H. Sykes, *Acc. Chem. Res.* **2019**, *52*, 237.

[146] S. Shin, J. Kim, S. Park, H.-E. Kim, Y.-E. Sung, H. Lee, *Chem. Commun.* **2019**, *55*, 6389.

[147] E. Luo, H. Zhang, X. Wang, L. Gao, L. Gong, T. Zhao, Z. Jin, J. Ge, Z. Jiang, C. Liu, W. Xing, *Angew. Chem. Int. Ed.* **2019**, *58*, 12469.

[148] J. Li, M. Chen, D. A. Cullen, S. Hwang, M. Wang, B. Li, K. Liu, S. Karakalos, M. Lucero, H. Zhang, C. Lei, H. Xu, G. E. Sterbinsky, Z. Feng, D. Su, K. L. More, G. Wang, Z. Wang, G. Wu, *Nat. Catal.* **2018**, *1*, 935.

[149] H. Zhang, S. Hwang, M. Wang, Z. Feng, S. Karakalos, L. Luo, Z. Qiao, X. Xie, C. Wang, D. Su, Y. Shao, G. Wu, *J. Am. Chem. Soc.* **2017**, *139*, 14143.

[150] J. Wu, H. Zhou, Q. Li, M. Chen, J. Wan, N. Zhang, L. Xiong, S. Li, B. Y. Xia, G. Feng, M. Liu, L. Huang, *Adv. Energy Mater.* **2019**, *9*, 1900149.

[151] V. Vij, S. Sultan, A. M. Harzandi, A. Meena, J. N. Tiwari, W.-G. Lee, T. Yoon, K. S. Kim, *ACS Catal.* **2017**, *7*, 7196.

[152] L. Cui, L. Cui, Z. Li, J. Zhang, H. Wang, S. Lu, Y. Xiang, *J. Mater. Chem. A* **2019**, *7*, 16690.

[153] J. Li, S. Chen, N. Yang, M. Deng, S. Ibraheem, J. Deng, J. Li, L. Li, Z. Wei, *Angew. Chem. Int. Ed.* **2019**, *58*, 7035.

[154] L. Cao, Q. Luo, J. Chen, L. Wang, Y. Lin, H. Wang, X. Liu, X. Shen, W. Zhang, W. Liu, Z. Qi, Z. Jiang, J. Yang, T. Yao, *Nat. Commun.* **2019**, *10*, 4849.

[155] D. Liu, J.-C. Li, S. Ding, Z. Lyu, S. Feng, H. Tian, C. Huyan, M. Xu, T. Li, D. Du, P. Liu, M. Shao, Y. Lin, *Small Methods* **2020**, *4*, 1900827.

[156] J. Wang, G. Han, L. Wang, L. Du, G. Chen, Y. Gao, Y. Ma, C. Du, X. Cheng, P. Zuo, G. Yin, *Small* **2018**, *14*, 1704282.

[157] X. Li, H. Rong, J. Zhang, D. Wang, Y. Li, *Nano Res.* **2020**, *13*, 1842.

[158] Y. Zhu, J. Sokolowski, X. Song, Y. He, Y. Mei, G. Wu, *Adv. Energy Mater.* **2020**, *10*, 1902844.

[159] Y. Gao, Z. Cai, X. Wu, Z. Lv, P. Wu, C. Cai, *ACS Catal.* **2018**, *8*, 10364.

[160] J. Chen, H. Li, C. Fan, Q. Meng, Y. Tang, X. Qiu, G. Fu, T. Ma, *Adv. Mater.* **2020**, *32*, 2003134.

[161] A. Zitolo, V. Goellner, V. Armel, M.-T. Sougrati, T. Mineva, L. Stievano, E. Fonda, F. Jaouen, *Nat. Mater.* **2015**, *14*, 937.

[162] H. T. Chung, D. A. Cullen, D. Higgins, B. T. Sneed, E. F. Holby, K. L. More, P. Zelenay, *Science* **2017**, *357*, 479.

[163] M. Xiao, J. Zhu, L. Ma, Z. Jin, J. Ge, X. Deng, Y. Hou, Q. He, J. Li, Q. Jia, S. Mukerjee, R. Yang, Z. Jiang, D. Su, C. Liu, W. Xing, *ACS Catal.* **2018**, *8*, 2824.

[164] H. Shen, E. Gracia-Espino, J. Ma, H. Tang, X. Mamat, T. Wagberg, G. Hu, S. Guo, *Nano Energy* **2017**, *35*, 9.

[165] Y. Cheng, S. He, S. Lu, J.-P. Veder, B. Johannessen, L. Thomsen, M. Saunders, T. Becker, R. De Marco, Q. Li, S.-z. Yang, S. P. Jiang, *Adv. Sci.* **2019**, *6*, 1802066.

[166] Z. Zhang, J. Sun, F. Wang, L. Dai, *Angew. Chem. Int. Ed.* **2018**, *57*, 9038.

[167] K. Yuan, D. Lützenkirchen-Hecht, L. Li, L. Shuai, Y. Li, R. Cao, M. Qiu, X. Zhuang, M. K. H. Leung, Y. Chen, U. Scherf, *J. Am. Chem. Soc.* **2020**, *142*, 2404.

[168] J. Zhang, Y. Zhao, C. Chen, Y.-C. Huang, C.-L. Dong, C.-J. Chen, R.-S. Liu, C. Wang, K. Yan, Y. Li, G. Wang, *J. Am. Chem. Soc.* **2019**, *141*, 20118.

[169] Y. Zhou, W. Yang, W. Utetiwabo, Y.-m. Lian, X. Yin, L. Zhou, P. Yu, R. Chen, S. Sun, *J. Phys. Chem. Lett.* **2020**, *11*, 1404.

[170] Y. Wang, Y.-J. Tang, K. Zhou, *J. Am. Chem. Soc.* **2019**, *141*, 14115.

[171] Y. Shao, J.-P. Dodelet, G. Wu, P. Zelenay, *Adv. Mater.* **2019**, *31*, 1807615.

[172] H. Zhang, X. F. Lu, Z.-P. Wu, X. W. D. Lou, *ACS Cent. Sci.* **2020**, *6*, 1288.

[173] Q. Zhang, J. Guan, *Adv. Funct. Mater.* **2020**, *30*, 2000768.

[174] Z. Du, X. Chen, W. Hu, C. Chuang, S. Xie, A. Hu, W. Yan, X. Kong, X. Wu, H. Ji, L.-J. Wan, *J. Am. Chem. Soc.* **2019**, *141*, 3977.

[175] T. Sun, S. Zhao, W. Chen, D. Zhai, J. Dong, Y. Wang, S. Zhang, A. Han, L. Gu, R. Yu, X. Wen, H. Ren, L. Xu, C. Chen, Q. Peng, D. Wang, Y. Li, *Proc. Natl. Acad. Sci. USA* **2018**, *115*, 12692.

[176] S. Nitopi, E. Bertheussen, S. B. Scott, X. Liu, A. K. Engstfeld, S. Horch, B. Seger, I. E. L. Stephens, K. Chan, C. Hahn, J. K. Nørskov, T. F. Jaramillo, I. Chorkendorff, *Chem. Rev.* **2019**, *119*, 7610.

[177] A. Bhagi-Damodaran, M. A. Michael, Q. Zhu, J. Reed, B. A. Sandoval, E. N. Mirts, S. Chakraborty, P. Moënne-Loccoz, Y. Zhang, Y. Lu, *Nat. Chem.* **2017**, *9*, 257.

[178] X.-F. Yang, A. Wang, B. Qiao, J. Li, J. Liu, T. Zhang, *Acc. Chem. Res.* **2013**, *46*, 1740.

[179] Y. Qu, Z. Li, W. Chen, Y. Lin, T. Yuan, Z. Yang, C. Zhao, J. Wang, C. Zhao, X. Wang, F. Zhou, Z. Zhuang, Y. Wu, Y. Li, *Nat. Catal.* **2018**, *1*, 781.

[180] F. Li, G.-F. Han, H.-J. Noh, S.-J. Kim, Y. Lu, H. Y. Jeong, Z. Fu, J.-B. Baek, *Energy Environ. Sci.* **2018**, *11*, 2263.

[181] P. Song, M. Luo, X. Liu, W. Xing, W. Xu, Z. Jiang, L. Gu, *Adv. Funct. Mater.* **2017**, *27*, 1700802.

[182] M. Xiao, J. Zhu, G. Li, N. Li, S. Li, Z. P. Cano, L. Ma, P. Cui, P. Xu, G. Jiang, H. Jin, S. Wang, T. Wu, J. Lu, A. Yu, D. Su, Z. Chen, *Angew. Chem. Int. Ed.* **2019**, *58*, 9640.

[183] X. Zhang, J. Guo, P. Guan, C. Liu, H. Huang, F. Xue, X. Dong, S. J. Pennycook, M. F. Chisholm, *Nat. Commun.* **2013**, *4*, 1924.

[184] Y. Hou, Y. Liu, R. Gao, Q. Li, H. Guo, A. Goswami, R. Zbořil, M. B. Gawande, X. Zou, *ACS Catal.* **2017**, *7*, 7038.

[185] S. Divanis, T. Kutlusoy, I. M. Ingmer Boye, I. C. Man, J. Rossmeisl, *Chem. Sci.* **2020**, *11*, 2943.

[186] E. Fabbri, T. J. Schmidt, *ACS Catal.* **2018**, *8*, 9765.

[187] Z. Shi, X. Wang, J. Ge, C. Liu, W. Xing, *Nanoscale* **2020**, *12*, 13249.

[188] Y. Lee, J. Suntivich, K. J. May, E. E. Perry, Y. Shao-Horn, *J. Phys. Chem. Lett.* **2012**, *3*, 399.

[189] Y. Lin, Z. Tian, L. Zhang, J. Ma, Z. Jiang, B. J. Deibert, R. Ge, L. Chen, *Nat. Commun.* **2019**, *10*, 162.

[190] Q. Shi, C. Zhu, D. Du, Y. Lin, *Chem. Soc. Rev.* **2019**, *48*, 3181.

[191] C. Zhu, Q. Shi, S. Feng, D. Du, Y. Lin, *ACS Energy Lett.* **2018**, *3*, 1713.

[192] Y.-Q. Su, Y. Wang, J.-X. Liu, I. A. W. Filot, K. Alexopoulos, L. Zhang, V. Muravev, B. Zijlstra, D. G. Vlachos, E. J. M. Hensen, *ACS Catal.* **2019**, *9*, 3289.

[193] S. Liang, C. Hao, Y. Shi, *ChemCatChem* **2015**, *7*, 2559.

[194] M. B. Gawande, P. Fornasiero, R. Zbořil, *ACS Catal.* **2020**, *10*, 2231.

[195] W. H. Lee, Y.-J. Ko, J.-Y. Kim, B. K. Min, Y. J. Hwang, H.-S. Oh, *Chem. Commun.* **2020**, *56*, 12687.

[196] Q. Liu, Z. Zhang, *Catal. Sci. Technol.* **2019**, *9*, 4821.

[197] L. Li, X. Chang, X. Lin, Z.-J. Zhao, J. Gong, *Chem. Soc. Rev.* **2020**, *49*, 8156.

[198] C. Dessal, T. Len, F. Morfin, J.-L. Rousset, M. Aouine, P. Afanasiev, L. Piccolo, *ACS Catal.* **2019**, *9*, 5752.

[199] C. Lin, Y. Zhao, H. Zhang, S. Xie, Y.-F. Li, X. Li, Z. Jiang, Z.-P. Liu, *Chem. Sci.* **2018**, *9*, 6803.

[200] P. Li, M. Wang, X. Duan, L. Zheng, X. Cheng, Y. Zhang, Y. Kuang, Y. Li, Q. Ma, Z. Feng, W. Liu, X. Sun, *Nat. Commun.* **2019**, *10*, 1711.

[201] Q.-Q. Chen, C.-C. Hou, C.-J. Wang, X. Yang, R. Shi, Y. Chen, *Chem. Commun.* **2018**, *54*, 6400.

[202] G. Chen, T. Wang, J. Zhang, P. Liu, H. Sun, X. Zhuang, M. Chen, X. Feng, *Adv. Mater.* **2018**, *30*, 1706279.

[203] J. Zhang, J. Liu, L. Xi, Y. Yu, N. Chen, S. Sun, W. Wang, K. M. Lange, B. Zhang, *J. Am. Chem. Soc.* **2018**, *140*, 3876.

[204] Z. Zhang, C. Feng, C. Liu, M. Zuo, L. Qin, X. Yan, Y. Xing, H. Li, R. Si, S. Zhou, J. Zeng, *Nat. Commun.* **2020**, *11*, 1215.

[205] W.-H. Lai, L.-F. Zhang, W.-B. Hua, S. Indris, Z.-C. Yan, Z. Hu, B. Zhang, Y. Liu, L. Wang, M. Liu, R. Liu, Y.-X. Wang, J.-Z. Wang, Z. Hu, H.-K. Liu, S.-L. Chou, S.-X. Dou, *Angew. Chem. Int. Ed.* **2019**, *58*, 11868.

[206] L. Zhuang, L. Ge, Y. Yang, M. Li, Y. Jia, X. Yao, Z. Zhu, *Adv. Mater.* **2017**, *29*, 1606793.

[207] C. Feng, M. B. Faheem, J. Fu, Y. Xiao, C. Li, Y. Li, *ACS Catal.* **2020**, *10*, 4019.

[208] R. Gusmão, M. Veselý, Z. Sofer, *ACS Catal.* **2020**, *10*, 9634.

[209] C. Ling, L. Shi, Y. Ouyang, X. C. Zeng, J. Wang, *NanoLett.* **2017**, *17*, 5133.

[210] R. Subbaraman, D. Tripkovic, K.-C. Chang, D. Strmcnik, A. P. Paulikas, P. Hirunsit, M. Chan, J. Greeley, V. Stamenkovic, N. M. Markovic, *Nat. Mater.* **2012**, *11*, 550.

[211] H. Xiao, H. Shin, W. A. Goddard, *Proc. Natl. Acad. Sci. USA* **2018**, *115*, 5872.

[212] J.-L. Shui, N. K. Karan, M. Balasubramanian, S.-Y. Li, D.-J. Liu, *J. Am. Chem. Soc.* **2012**, *134*, 16654.

[213] B. Wurster, D. Grumelli, D. Hötger, R. Gutzler, K. Kern, *J. Am. Chem. Soc.* **2016**, *138*, 3623.

[214] C. C. L. McCrory, S. Jung, J. C. Peters, T. F. Jaramillo, *J. Am. Chem. Soc.* **2013**, *135*, 16977.

[215] H. Fei, J. Dong, Y. Feng, C. S. Allen, C. Wan, B. Volosskiy, M. Li, Z. Zhao, Y. Wang, H. Sun, P. An, W. Chen, Z. Guo, C. Lee, D. Chen, I. Shakir, M. Liu, T. Hu, Y. Li, A. I. Kirkland, X. Duan, Y. Huang, *Nat. Catal.* **2018**, *1*, 63.

[216] L. Bai, C.-S. Hsu, D. T. L. Alexander, H. M. Chen, X. Hu, *J. Am. Chem. Soc.* **2019**, *141*, 14190.

[217] S. Sultan, J. N. Tiwari, A. N. Singh, S. Zhumagali, M. Ha, C. W. Myung, P. Thangavel, K. S. Kim, *Adv. Energy Mater.* **2019**, *9*, 1900624.

[218] J. Kim, C.-W. Roh, S. K. Sahoo, S. Yang, J. Bae, J. W. Han, H. Lee, *Adv. Energy Mater.* **2018**, *8*, 1701476.

[219] S. Singh, S. Jain, V. Ps, A. K. Tiwari, M. R. Nouni, J. K. Pandey, S. Goel, *Renew. Sustain. Energy Rev.* **2015**, *51*, 623.

[220] S. Mitchell, J. Pérez-Ramírez, *Nat. Commun.* **2020**, *11*, 4302.

[221] J. Wu, N. Han, S. Ning, T. Chen, C. Zhu, C. Pan, H. Wu, S. J. Pennycook, C. Guan, *ACS Sustain. Chem. Eng.* **2020**, *8*, 14825.

[222] Q. He, D. Tian, H. Jiang, D. Cao, S. Wei, D. Liu, P. Song, Y. Lin, L. Song, *Adv. Mater.* **2020**, *32*, 1906972.

[223] J. Wang, F. Xu, H. Jin, Y. Chen, Y. Wang, *Adv. Mater.* **2017**, *29*, 1605838.

[224] X. Li, X. Yang, Y. Huang, T. Zhang, B. Liu, *Adv. Mater.* **2019**, *31*, 1902031.

[225] N. Mahmood, Y. Yao, J.-W. Zhang, L. Pan, X. Zhang, J.-J. Zou, *Adv. Sci.* **2018**, *5*, 1700464.

[226] H. Liu, X. Peng, X. Liu, *ChemElectroChem* **2018**, *5*, 2963.

[227] W. Zang, Z. Kou, S. J. Pennycook, J. Wang, *Adv. Energy Mater.* **2020**, *10*, 1903181.

[228] B. Bayatsarmadi, Y. Zheng, A. Vasileff, S.-Z. Qiao, *Small* **2017**, *13*, 1700191.

[229] H. Zhang, P. An, W. Zhou, B. Y. Guan, P. Zhang, J. Dong, X. W. Lou, *Sci. Adv.* **2018**, *4*, 6657.

[230] T. Li, J. Liu, Y. Song, F. Wang, *ACS Catal.* **2018**, *8*, 8450.

[231] L. Cao, Q. Luo, W. Liu, Y. Lin, X. Liu, Y. Cao, W. Zhang, Y. Wu, J. Yang, T. Yao, S. Wei, *Nat. Catal.* **2019**, *2*, 134.

[232] C. Li, J.-B. Baek, *ACS Omega* **2020**, *5*, 31.

[233] X.-P. Yin, H.-J. Wang, S.-F. Tang, X.-L. Lu, M. Shu, R. Si, T.-B. Lu, *Angew. Chem. Int. Ed.* **2018**, *57*, 9382.

[234] S. K. Sahoo, Y. Ye, S. Lee, J. Park, H. Lee, J. Lee, J. W. Han, *ACS Energy Lett.* **2019**, *4*, 126.

[235] Q. Cheng, C. Hu, G. Wang, Z. Zou, H. Yang, L. Dai, *J. Am. Chem. Soc.* **2020**, *142*, 5594.

[236] K. Jiang, B. Liu, M. Luo, S. Ning, M. Peng, Y. Zhao, Y.-R. Lu, T.-S. Chan, F. M. F. de Groot, Y. Tan, *Nat. Commun.* **2019**, *10*, 1743.

[237] Y. Wang, J. Mao, X. Meng, L. Yu, D. Deng, X. Bao, *Chem. Rev.* **2019**, *119*, 1806.

[238] N. Xuan, J. Chen, J. Shi, Y. Yue, P. Zhuang, K. Ba, Y. Sun, J. Shen, Y. Liu, B. Ge, Z. Sun, *Chem. Mater.* **2019**, *31*, 429.

[239] M. Sun, J. Ji, M. Hu, M. Weng, Y. Zhang, H. Yu, J. Tang, J. Zheng, Z. Jiang, F. Pan, C. Liang, Z. Lin, *ACS Catal.* **2019**, *9*, 8213.

[240] V. Ramalingam, P. Varadhan, H.-C. Fu, H. Kim, D. Zhang, S. Chen, L. Song, D. Ma, Y. Wang, H. N. Alshareef, J.-H. He, *Adv. Mater.* **2019**, *31*, 1903841.

[241] J. Zhang, X. Xu, L. Yang, D. Cheng, D. Cao, *Small Methods* **2019**, *3*, 1900653.

[242] B. Lu, L. Guo, F. Wu, Y. Peng, J. E. Lu, T. J. Smart, N. Wang, Y. Z. Finfrock, D. Morris, P. Zhang, N. Li, P. Gao, Y. Ping, S. Chen, *Nat. Commun.* **2019**, *10*, 631.

[243] Y. Li, F. Chu, Y. Liu, Y. Kong, Y. Tao, Y. Li, Y. Qin, *Chem. Commun.* **2018**, *54*, 13076.

[244] F. Luo, H. Hu, X. Zhao, Z. Yang, Q. Zhang, J. Xu, T. Kaneko, Y. Yoshida, C. Zhu, W. Cai, *Nano Lett.* **2020**, *20*, 2120.

[245] Z. Li, J.-Y. Fu, Y. Feng, C.-K. Dong, H. Liu, X.-W. Du, *Nat. Catal.* **2019**, *2*, 1107.

[246] J. Yang, Y. Wang, M. J. Lagos, V. Manichev, R. Fullon, X. Song, D. Voiry, S. Chakraborty, W. Zhang, P. E. Batson, L. Feldman, T. Gustafsson, M. Chhowalla, *ACS Nano* **2019**, *13*, 9958.

[247] K. Qi, X. Cui, L. Gu, S. Yu, X. Fan, M. Luo, S. Xu, N. Li, L. Zheng, Q. Zhang, J. Ma, Y. Gong, F. Lv, K. Wang, H. Huang, W. Zhang, S. Guo, W. Zheng, P. Liu, *Nat. Commun.* **2019**, *10*, 5231.

[248] L. Zhang, R. Si, H. Liu, N. Chen, Q. Wang, K. Adair, Z. Wang, J. Chen, Z. Song, J. Li, M. N. Banis, R. Li, T.-K. Sham, M. Gu, L.-M. Liu, G. A. Botton, X. Sun, *Nat. Commun.* **2019**, *10*, 4936.

[249] Y. Xue, B. Huang, Y. Yi, Y. Guo, Z. Zuo, Y. Li, Z. Jia, H. Liu, Y. Li, *Nat. Commun.* **2018**, *9*, 1460.

[250] B. D. Matson, J. C. Peters, *ACS Catal.* **2018**, *8*, 1448.

[251] C. Tang, R. Zhang, W. Lu, L. He, X. Jiang, A. M. Asiri, X. Sun, *Adv. Mater.* **2017**, *29*, 1602441.

[252] L. Wang, X. Liu, L. Cao, W. Zhang, T. Chen, Y. Lin, H. Wang, Y. Wang, T. Yao, *J. Phys. Chem. Lett.* **2020**, *11*, 6691.

[253] W. Lai, H. Wang, L. Zheng, Q. Jiang, Z.-C. Yan, L. Wang, H. Yoshikawa, D. Matsumura, Q. Sun, Y.-X. Wang, Q. Gu, J.-Z. Wang, H.-K. Liu, S. Chou, S.-X. Dou, *Angew. Chem. Int. Ed.* **2020**, *59*, 22171.

[254] Y. Jiao, Y. Zheng, K. Davey, S.-Z. Qiao, *Nat. Energy* **2016**, *1*, 16130.

[255] H. Fei, J. Dong, M. J. Arellano-Jiménez, G. Ye, N. Dong Kim, E. L. G. Samuel, Z. Peng, Z. Zhu, F. Qin, J. Bao, M. J. Yacaman, P. M. Ajayan, D. Chen, J. M. Tour, *Nat. Commun.* **2015**, *6*, 8668.

[256] J.-D. Yi, R. Xu, G.-L. Chai, T. Zhang, K. Zang, B. Nan, H. Lin, Y.-L. Liang, J. Lv, J. Luo, R. Si, Y.-B. Huang, R. Cao, *J. Mater. Chem. A* **2019**, *7*, 1252.

[257] L. Peng, L. Shang, T. Zhang, G. I. N. Waterhouse, *Adv. Energy Mater.* **2020**, 2003018, https://doi.org/10.1002/aenm.202003018.

[258] L. Fang, Z. Feng, L. Cheng, R. E. Winans, T. Li, *Small Methods* **2020**, *4*, 2000315.

[259] D. Zhang, S. Wang, R. Hu, J. Gu, Y. Cui, B. Li, W. Chen, C. Liu, J. Shang, S. Yang, *Adv. Funct. Mater.* **2020**, *30*, 2002471.

[260] Z. Lin, H. Huang, L. Cheng, Y. Yang, R. Zhang, Q. Chen, *ACS Sustain. Chem. Eng.* **2020**, *8*, 427.

[261] L. Li, Z.-w. Chang, X.-B. Zhang, *Adv. Sustain. Syst.* **2017**, *1*, 1700036.

[262] R. Cao, J.-S. Lee, M. Liu, J. Cho, *Adv. Energy Mater.* **2012**, *2*, 816.

[263] D. U. Lee, P. Xu, Z. P. Cano, A. G. Kashkooli, M. G. Park, Z. Chen, *J. Mater. Chem. A* **2016**, *4*, 7107.

[264] X. Liu, L. Dai, *Nat. Rev. Mater.* **2016**, *1*, 16064.

[265] Z. Zhao, M. Li, L. Zhang, L. Dai, Z. Xia, *Adv. Mater.* **2015**, *27*, 6834.

[266] H.-F. Wang, C. Tang, Q. Zhang, *Adv. Funct. Mater.* **2018**, *28*, 1803329.

[267] Y. Huang, Y. Wang, C. Tang, J. Wang, Q. Zhang, Y. Wang, J. Zhang, *Adv. Mater.* **2019**, *31*, 1803800.

[268] A. Han, B. Wang, A. Kumar, Y. Qin, J. Jin, X. Wang, C. Yang, B. Dong, Y. Jia, J. Liu, X. Sun, *Small Methods* **2019**, *3*, 1800471.

[269] Y. Zhong, Y. Xu, W. Wang, Z. Shao, *Batteries Supercaps* **2019**, *2*, 272.

[270] J. Fu, R. Liang, G. Liu, A. Yu, Z. Bai, L. Yang, Z. Chen, *Adv. Mater.* **2019**, *31*, 1805230.

[271] B.-W. Zhang, Y.-X. Wang, S.-L. Chou, H.-K. Liu, S.-X. Dou, *Small Methods* **2019**, *3*, 1800497.

[272] W.-H. Lai, Z. Miao, Y.-X. Wang, J.-Z. Wang, S.-L. Chou, *Adv. Energy Mater.* **2019**, *9*, 1900722.

[273] L. Yang, L. Shi, D. Wang, Y. Lv, D. Cao, *Nano Energy* **2018**, *50*, 691.

[274] W. Zang, A. Sumboja, Y. Ma, H. Zhang, Y. Wu, S. Wu, H. Wu, Z. Liu, C. Guan, J. Wang, S. J. Pennycook, *ACS Catal.* **2018**, *8*, 8961.

[275] S. Ren, X. Duan, S. Liang, M. Zhang, H. Zheng, *J. Mater. Chem. A* **2020**, *8*, 6144.

[276] L. Wang, Y. Wang, M. Wu, Z. Wei, C. Cui, M. Mao, J. Zhang, X. Han, Q. Liu, J. Ma, *Small* **2018**, *14*, 1800737.

[277] P. Chen, T. Zhou, L. Xing, K. Xu, Y. Tong, H. Xie, L. Zhang, W. Yan, W. Chu, C. Wu, Y. Xie, *Angew. Chem. Int. Ed.* **2017**, *56*, 610.

[278] J. Han, X. Meng, L. Lu, J. Bian, Z. Li, C. Sun, *Adv. Funct. Mater.* **2019**, *29*, 1808872.

[279] Y. Chen, S. Ji, S. Zhao, W. Chen, J. Dong, W.-C. Cheong, R. Shen, X. Wen, L. Zheng, A. I. Rykov, S. Cai, H. Tang, Z. Zhuang, C. Chen, Q. Peng, D. Wang, Y. Li, *Nat. Commun.* **2018**, *9*, 5422.

[280] Z. K. Yang, C.-Z. Yuan, A.-W. Xu, *ACS Energy Lett.* **2018**, *3*, 2383.

[281] P. Peng, L. Shi, F. Huo, C. Mi, X. Wu, S. Zhang, Z. Xiang, *Sci. Adv.* **2019**, *5*, 2322.

[282] J. Zhang, M. Zhang, Y. Zeng, J. Chen, L. Qiu, H. Zhou, C. Sun, Y. Yu, C. Zhu, Z. Zhu, *Small* **2019**, *15*, 1900307.

[283] H. Sun, S. Liu, M. Wang, T. Qian, J. Xiong, C. Yan, *ACS Appl. Mater. Interfaces* **2019**, *11*, 33054.

[284] Y. Pan, S. Liu, K. Sun, X. Chen, B. Wang, K. Wu, X. Cao, W.-C. Cheong, R. Shen, A. Han, Z. Chen, L. Zheng, J. Luo, Y. Lin, Y. Liu, D. Wang, Q. Peng, Q. Zhang, C. Chen, Y. Li, *Angew. Chem. Int. Ed.* **2018**, *57*, 8614.

[285] S. Li, C. Cheng, X. Zhao, J. Schmidt, A. Thomas, *Angew. Chem. Int. Ed.* **2018**, *57*, 1856.

[286] J. Li, H. Liu, M. Wang, C. Lin, W. Yang, J. Meng, Y. Xu, K. A. Owusu, B. Jiang, C. Chen, D. Fan, L. Zhou, L. Mai, *Chem. Commun.* **2019**, *55*, 334.

[287] B.-Q. Li, C.-X. Zhao, S. Chen, J.-N. Liu, X. Chen, L. Song, Q. Zhang, *Adv. Mater.* **2019**, *31*, 1900592.

[288] Y. Li, R. Cao, L. Li, X. Tang, T. Chu, B. Huang, K. Yuan, Y. Chen, *Small* **2020**, *16*, 1906735.

[289] Y. Wang, B. Yu, K. Liu, X. Yang, M. Liu, T.-S. Chan, X. Qiu, J. Li, W. Li, *J. Mater. Chem. A* **2020**, *8*, 2131.

[290] P. Yu, L. Wang, F. Sun, Y. Xie, X. Liu, J. Ma, X. Wang, C. Tian, J. Li, H. Fu, *Adv. Mater.* **2019**, *31*, 1901666.

[291] X. Han, X. Ling, Y. Wang, T. Ma, C. Zhong, W. Hu, Y. Deng, *Angew. Chem. Int. Ed.* **2019**, *58*, 5359.

[292] D. Ji, L. Fan, L. Li, S. Peng, D. Yu, J. Song, S. Ramakrishna, S. Guo, *Adv. Mater.* **2019**, *31*, 1808267.

[293] M. Yan, Y. Kawamata, P. S. Baran, *Chem. Rev.* **2017**, *117*, 13230.

[294] K. Mitsudo, Y. Kurimoto, K. Yoshioka, S. Suga, *Chem. Rev.* **2018**, *118*, 5985.

[295] K. D. Moeller, *Chem. Rev.* **2018**, *118*, 4817.

[296] G. Hilt, *ChemElectroChem* **2020**, *7*, 395.

[297] M. Yan, Y. Kawamata, P. S. Baran, *Angew. Chem. Int. Ed.* **2018**, *57*, 4149.

[298] A. Wiebe, T. Gieshoff, S. Möhle, E. Rodrigo, M. Zirbes, S. R. Waldvogel, *Angew. Chem. Int. Ed.* **2018**, *57*, 5594.

[299] B. A. Frontana-Uribe, R. D. Little, J. G. Ibanez, A. Palma, R. Vasquez-Medrano, *Green Chem.* **2010**, *12*, 2099.

[300] H. Wang, X. Gao, Z. Lv, T. Abdelilah, A. Lei, *Chem. Rev.* **2019**, *119*, 6769.

[301] M. D. Kärkäs, *Chem. Soc. Rev.* **2018**, *47*, 5786.

[302] C. Ma, P. Fang, T.-S. Mei, *ACS Catal.* **2018**, *8*, 7179.

[303] Y. Zhao, W. Xia, *Chem. Soc. Rev.* **2018**, *47*, 2591.

[304] R. Francke, R. D. Little, *Chem. Soc. Rev.* **2014**, *43*, 2492.

[305] S. R. Waldvogel, M. Selt, *Angew. Chem. Int. Ed.* **2016**, *55*, 12578.

[306] J. Zhou, X.-Z. Tao, J.-J. Dai, C.-G. Li, J. Xu, H.-M. Xu, H.-J. Xu, *Chem. Commun.* **2019**, *55*, 9208.

[307] E. J. Horn, B. R. Rosen, P. S. Baran, *ACS Cent. Sci.* **2016**, *2*, 302.

[308] H. Yan, C. Su, J. He, W. Chen, *J. Mater. Chem. A* **2018**, *6*, 8793.

[309] Y. Yuan, A. Lei, *Acc. Chem. Res.* **2019**, *52*, 3309.

[310] Y. Yuan, Y. Chen, S. Tang, Z. Huang, A. Lei, *Sci. Adv.* **2018**, *4*, 5312.

[311] K.-J. Jiao, Y.-K. Xing, Q.-L. Yang, H. Qiu, T.-S. Mei, *Acc. Chem. Res.* **2020**, *53*, 300.

[312] L. Ackermann, *Acc. Chem. Res.* **2020**, *53*, 84.

[313] W.-J. Kong, L. H. Finger, A. M. Messinis, R. Kuniyil, J. C. A. Oliveira, L. Ackermann, *J. Am. Chem. Soc.* **2019**, *141*, 17198.

[314] Y. Qiu, A. Scheremetjew, L. Ackermann, *J. Am. Chem. Soc.* **2019**, *141*, 2731.

[315] Y. Wang, L. Deng, X. Wang, Z. Wu, Y. Wang, Y. Pan, *ACS Catal.* **2019**, *9*, 1630.

[316] Y. Yuan, Y. Cao, Y. Lin, Y. Li, Z. Huang, A. Lei, *ACS Catal.* **2018**, *8*, 10871.

[317] D. Wang, P. Wang, S. Wang, Y.-H. Chen, H. Zhang, A. Lei, *Nat. Commun.* **2019**, *10*, 2796.

[318] N. Fu, G. S. Sauer, A. Saha, A. Loo, S. Lin, *Science* **2017**, *357*, 575.

[319] N. Fu, Y. Shen, A. R. Allen, L. Song, A. Ozaki, S. Lin, *ACS Catal.* **2019**, *9*, 746.

[320] Q.-L. Yang, Y.-K. Xing, X.-Y. Wang, H.-X. Ma, X.-J. Weng, X. Yang, H.-M. Guo, T.-S. Mei, *J. Am. Chem. Soc.* **2019**, *141*, 18970.

[321] X. Huang, Q. Zhang, J. Lin, K. Harms, E. Meggers, *Nat. Catal.* **2019**, *2*, 34.

[322] Q.-L. Yang, X.-Y. Wang, J.-Y. Lu, L.-P. Zhang, P. Fang, T.-S. Mei, *J. Am. Chem. Soc.* **2018**, *140*, 11487.

[323] R. Mei, N. Sauermann, J. C. A. Oliveira, L. Ackermann, *J. Am. Chem. Soc.* **2018**, *140*, 7913.

[324] B. G. Hashiguchi, S. M. Bischof, M. M. Konnick, R. A. Periana, *Acc. Chem. Res.* **2012**, *45*, 885.

[325] F. Zaera, *ACS Catal.* **2017**, *7*, 4947.

[326] J. A. Labinger, J. E. Bercaw, *Nature* **2002**, *417*, 507.

[327] T. G. Saint-Denis, R.-Y. Zhu, G. Chen, Q.-F. Wu, J.-Q. Yu, *Science* **2018**, *359*, 4798.

[328] D. Li, X. Li, J. Gong, *Chem. Rev.* **2016**, *116*, 11529.

[329] W. Liu, L. Zhang, W. Yan, X. Liu, X. Yang, S. Miao, W. Wang, A. Wang, T. Zhang, *Chem. Sci.* **2016**, *7*, 5758.

[330] X. Cui, K. Junge, X. Dai, C. Kreyenschulte, M.-M. Pohl, S. Wohlrab, F. Shi, A. Brückner, M. Beller, *ACS Cent. Sci.* **2017**, *3*, 580.

[331] W. Liu, L. Zhang, X. Liu, X. Liu, X. Yang, S. Miao, W. Wang, A. Wang, T. Zhang, *J. Am. Chem. Soc.* **2017**, *139*, 10790.

[332] D. Huang, G. A. de Vera, C. Chu, Q. Zhu, E. Stavitski, J. Mao, H. Xin, J. A. Spies, C. A. Schmuttenmaer, J. Niu, G. L. Haller, J.-H. Kim, *ACS Catal.* **2018**, *8*, 9353.

[333] Y. Lou, Y. Zheng, X. Li, N. Ta, J. Xu, Y. Nie, K. Cho, J. Liu, *J. Am. Chem. Soc.* **2019**, *141*, 19289.

[334] J. Zhang, C. Zheng, M. Zhang, Y. Qiu, Q. Xu, W.-C. Cheong, W. Chen, L. Zheng, L. Gu, Z. Hu, D. Wang, Y. Li, *Nano Res.* **2020**, *13*, 3082.

[335] X. He, Q. He, Y. Deng, M. Peng, H. Chen, Y. Zhang, S. Yao, M. Zhang, D. Xiao, D. Ma, B. Ge, H. Ji, *Nat. Commun.* **2019**, *10*, 3663.

[336] Y. Ma, Y. Ren, Y. Zhou, W. Liu, W. Baaziz, O. Ersen, C. Pham-Huu, M. Greiner, W. Chu, A. Wang, T. Zhang, Y. Liu, *Angew. Chem. Int. Ed.* **2020**, *59*, 21613.

[337] M. Borrome, S. Gronert, *Angew. Chem. Int. Ed.* **2019**, *58*, 14906.

[338] Q. Wan, V. Fung, S. Lin, Z. Wu, D.-e. Jiang, *J. Mater. Chem. A* **2020**, *8*, 4362.

[339] G. Sun, Z.-J. Zhao, R. Mu, S. Zha, L. Li, S. Chen, K. Zang, J. Luo, Z. Li, S. C. Purdy, A. J. Kropf, J. T. Miller, L. Zeng, J. Gong, *Nat. Commun.* **2018**, *9*, 4454.

[340] Y. Nakaya, J. Hirayama, S. Yamazoe, K.-i. Shimizu, S. Furukawa, *Nat. Commun.* **2020**, *11*, 2838.

[341] Y. Pan, Y. Chen, K. Wu, Z. Chen, S. Liu, X. Cao, W.-C. Cheong, T. Meng, J. Luo, L. Zheng, C. Liu, D. Wang, Q. Peng, J. Li, C. Chen, *Nat. Commun.* **2019**, *10*, 4290.

[342] X. Long, Z. Li, G. Gao, P. Sun, J. Wang, B. Zhang, J. Zhong, Z. Jiang, F. Li, *Nat. Commun.* **2020**, *11*, 4074.

[343] Z. Chen, E. Vorobyeva, S. Mitchell, E. Fako, M. A. Ortuño, N. López, S. M. Collins, P. A. Midgley, S. Richard, G. Vilé, J. Pérez-Ramírez, *Nat. Nanotechnol.* **2018**, *13*, 702.

[344] G. Zhou, S. Zhao, T. Wang, S.-Z. Yang, B. Johannessen, H. Chen, C. Liu, Y. Ye, Y. Wu, Y. Peng, C. Liu, S. P. Jiang, Q. Zhang, Y. Cui, *Nano Lett.* **2020**, *20*, 1252.

[345] H.-Y. Zhuo, X. Zhang, J.-X. Liang, Q. Yu, H. Xiao, J. Li, *Chem. Rev.* **2020**, *120*, 12315.

[346] N. Kong, X. Fan, F. Liu, L. Wang, H. Lin, Y. Li, S.-T. Lee, *ACS Nano* **2020**, *14*, 5772.

[347] J. Meng, J. Li, J. Liu, X. Zhang, G. Jiang, L. Ma, Z.-Y. Hu, S. Xi, Y. Zhao, M. Yan, P. Wang, X. Liu, Q. Li, J. Z. Liu, T. Wu, L. Mai, *ACS Cent. Sci.* **2020**, *6*, 1431.

[348] J. Long, X. Fu, J. Xiao, *J. Mater. Chem. A* **2020**, *8*, 17078.

[349] H.-C. Huang, Y. Zhao, J. Wang, J. Li, J. Chen, Q. Fu, Y.-X. Bu, S.-B. Cheng, *J. Mater. Chem. A* **2020**, *8*, 9202.

[350] J.-C. Liu, Y.-G. Wang, J. Li, *J. Am. Chem. Soc.* **2017**, *139*, 6190.

[351] M. D. Hossain, Z. Liu, M. Zhuang, X. Yan, G.-L. Xu, C. A. Gadre, A. Tyagi, I. H. Abidi, C.-J. Sun, H. Wong, A. Guda, Y. Hao, X. Pan, K. Amine, Z. Luo, *Adv. Energy Mater.* **2019**, *9*, 1803689.

[352] J. Gao, H. b. Yang, X. Huang, S.-F. Hung, W. Cai, C. Jia, S. Miao, H. M. Chen, X. Yang, Y. Huang, T. Zhang, B. Liu, *Chem* **2020**, *6*, 658.

[353] J. Huo, L. Lu, Z. Shen, Y. Liu, J. Guo, Q. Liu, Y. Wang, H. Liu, M. Wu, G. Wang, *J. Mater. Chem. A* **2020**, *8*, 16271.

[354] C. Gao, J. Low, R. Long, T. Kong, J. Zhu, Y. Xiong, *Chem. Rev.* **2020**, *120*, 12175.

[355] R. Qin, K. Liu, Q. Wu, N. Zheng, *Chem. Rev.* **2020**, *120*, 11810.

[356] G. Han, Y. Zheng, X. Zhang, Z. Wang, Y. Gong, C. Du, M. N. Banis, Y.-M. Yiu, T.-K. Sham, L. Gu, Y. Sun, Y. Wang, J. Wang, Y. Gao, G. Yin, X. Sun, *Nano Energy* **2019**, *66*, 104088.

[357] S. Cao, Y. Zhao, S. Lee, S. Yang, J. Liu, G. Giannakakis, M. Li, M. Ouyang, D. Wang, E. C. H. Sykes, M. Flytzani-Stephanopoulos, *Sci. Adv.* **2020**, *6*, 3809.

[358] L. Wang, W. Zhang, S. Wang, Z. Gao, Z. Luo, X. Wang, R. Zeng, A. Li, H. Li, M. Wang, X. Zheng, J. Zhu, W. Zhang, C. Ma, R. Si, J. Zeng, *Nat. Commun.* **2016**, *7*, 14036.

[359] L. Zhao, Y. Zhang, L.-B. Huang, X.-Z. Liu, Q.-H. Zhang, C. He, Z.-Y. Wu, L.-J. Zhang, J. Wu, W. Yang, L. Gu, J.-S. Hu, L.-J. Wan, *Nat. Commun.* **2019**, *10*, 1278.

[360] Y. Cheng, S. Zhao, B. Johannessen, J.-P. Veder, M. Saunders, M. R. Rowles, M. Cheng, C. Liu, M. F. Chisholm, R. De Marco, H.-M. Cheng, S.-Z. Yang, S. P. Jiang, *Adv. Mater.* **2018**, *30*, 1706287.

[361] D. Kunwar, S. Zhou, A. DeLaRiva, E. J. Peterson, H. Xiong, X. I. Pereira-Hernández, S. C. Purdy, R. ter Veen, H. H. Brongersma, J. T. Miller, H. Hashiguchi, L. Kovarik, S. Lin, H. Guo, Y. Wang, A. K. Datye, *ACS Catal.* **2019**, *9*, 3978.

[362] J. Shin, Y. J. Lee, A. Jan, S. M. Choi, M. Y. Park, S. Choi, J. Y. Hwang, S. Hong, S. G. Park, H. J. Chang, M. K. Cho, J. P. Singh, K. H. Chae, S. Yang, H.-I. Ji, H. Kim, J.-W. Son, J.-H. Lee, B.-K. Kim, H.-W. Lee, J. Hong, Y. J. Lee, K. J. Yoon, *Energy Environ. Sci.* **2020**, *13*, 4903.

[363] Z. Zhang, Y. Zhu, H. Asakura, B. Zhang, J. Zhang, M. Zhou, Y. Han, T. Tanaka, A. Wang, T. Zhang, N. Yan, *Nat. Commun.* **2017**, *8*, 16100.

[364] Y. Yao, Z. Huang, P. Xie, L. Wu, L. Ma, T. Li, Z. Pang, M. Jiao, Z. Liang, J. Gao, Y. He, D. J. Kline, M. R. Zachariah, C. Wang, J. Lu, T. Wu, T. Li, C. Wang, R. Shahbazian-Yassar, L. Hu, *Nat. Nanotechnol.* **2019**, *14*, 851.

[365] J. Jones, H. Xiong, A. T. DeLaRiva, E. J. Peterson, H. Pham, S. R. Challa, G. Qi, S. Oh, M. H. Wiebenga, X. I. Pereira Hernández, Y. Wang, A. K. Datye, *Science* **2016**, *353*, 150.

[366] H. Xu, Z. Zhang, J. Liu, C.-L. Do-Thanh, H. Chen, S. Xu, Q. Lin, Y. Jiao, J. Wang, Y. Wang, Y. Chen, S. Dai, *Nat. Commun.* **2020**, *11*, 3908.

[367] D. Yan, J. Chen, H. Jia, *Angew. Chem. Int. Ed.* **2020**, *59*, 13562.

[368] G. S. Parkinson, *Catal. Lett.* **2019**, *149*, 1137.

[369] H. Jeong, S. Shin, H. Lee, *ACS Nano* **2020**, *14*, 14355.

[370] W. D. Jones, *J. Am. Chem. Soc.* **2020**, *142*, 4955.

[371] J. Yang, Z. Qiu, C. Zhao, W. Wei, W. Chen, Z. Li, Y. Qu, J. Dong, J. Luo, Z. Li, Y. Wu, *Angew. Chem. Int. Ed.* **2018**, *57*, 14095.

[372] Y. Cheng, S. Yang, S. P. Jiang, S. Wang, *Small Methods* **2019**, *3*, 1800440.

[373] S. Voskian, T. A. Hatton, *Energy Environ. Sci.* **2019**, *12*, 3530.

[374] J. H. Rheinhardt, P. Singh, P. Tarakeshwar, D. A. Buttry, *ACS Energy Lett.* **2017**, *2*, 454.

[375] W. I. Al Sadat, L. A. Archer, *Sci. Adv.* **2016**, *2*, 1600968.

[376] S. Hoang, Y. Guo, A. J. Binder, W. Tang, S. Wang, J. Liu, H. Tran, X. Lu, Y. Wang, Y. Ding, E. A. Kyriakidou, J. Yang, T. J. Toops, T. R. Pauly, R. Ramprasad, P.-X. Gao, *Nat. Commun.* **2020**, *11*, 1062.

[377] L. Zhang, J. Zhang, M. Qi, X. Guo, X. Feng, *Energy Fuels* **2020**, *34*, 12792.

[378] S. De Corte, T. Hennebel, J. P. Fitts, T. Sabbe, V. Bliznuk, S. Verschuere, D. van der Lelie, W. Verstraete, N. Boon, *Environ. Sci. Technol.* **2011**, *45*, 8506.

Baljeet Singh received his Ph.D. in Chemical Science from Tata Institute of Fundamental Research (TIFR), Mumbai, India in 2017. His Ph.D. research was focused on the synthesis and development of solid adsorbents and their applications in CO_2 capture technology. He subsequently moved as a postdoctoral researcher, first to the Tata Institute of Fundamental Research, Hyderabad, India and then to CICECO-Aveiro Institute of Materials, Portugal. Dr. Singh's research interest has focused on the synthesis of stable amine adsorbents for direct CO_2 capture, VOC removal, and SACs.

Paolo Fornasiero obtained the degree in Chemistry In 1992 and the Ph.D. in heterogeneous catalysis in 1997 both at the University of Trieste (Italy). After one year as postdoctoral fellow at the Catalysis Research Center of the University of Reading (U.K.), in 1998 he was appointed Assistant Professor, in 2006 Associate Professor, and in 2016 Full Professor in Inorganic Chemistry at the University of Trieste. Prof. Fornasiero is Associate Researcher of the National Council of Research (CNR) and from 2008 he is the scientific responsible of the CNR Research Unit associated with the Institute of Chemistry of OrganoMetallic Compounds (ICCOM) of Florence and located at the University of Trieste – Department of Chemical and Pharmaceutical Sciences. Since February 2015 he is Associate Editor of ACS catalysis.

Radek Zbořil received his Ph.D. degree at the Palacký University Olomouc, Czech Republic. After his doctoral studies, he spent some time at universities around the world in locations such as Tokyo, Delaware, and Johannesburg. Currently, he is a General Director of the Regional Centre of Advanced Technologies and Materials and a Professor at the Palacký University Olomouc, Czech Republic. His research interests focus on nanomaterial research for applications in catalysis, water treatment, antimicrobial technologies, medicine, energy storage, and biotechnology. He is an author of more than 550 scientific papers with more than 25 000 citations.

Manoj B. Gawande received his Ph.D. in 2008 from the Institute of Chemical Technology, Mumbai, India and then undertook several research stints in Germany, South Korea, Portugal, Czech Republic, USA, and UK. He also worked as a Visiting Professor at CBC-SPMS, Nanyang Technological University, Singapore in 2013. Presently, he is Associate Professor at the Institute of Chemical Technology-Mumbai Marathwada Campus, Jalna, India. His research interests focus on SACs, advanced nanomaterials, sustainable technologies, and cutting-edge catalysis and energy applications. Currently, he is supervising several doctoral students and postdoctoral co-workers. He has published over 115 international scientific papers.